Neuraminidase inhibitors rewire neutrophil function in murine sepsis and COVID-19 patients' cells

Rodrigo O. Formiga[1,2], Flávia C. Amaral[1,2], Camila F. Souza[2], Daniel A. G. B. Mendes[1,2], Carlos W. S. Wanderley[3], Cristina B. Lorenzini[1,2], Adara A. Santos[1,4], Juliana Antônia[1], Lucas F. Faria[1], Caio C. Natale[1,2], Nicholas M. Paula[1,2], Priscila C. S. Silva[1], Fernanda R. Fonseca[5], Luan Aires[1,2], Nicoli Heck[1], Shana P. C. Barroso[6], Alexandre Morrot[7], Regina Sordi[2], Frederico Alisson-Silva[8], Daniel S. Mansur[1,4], Fernando Q. Cunha[3], Rosemeri Maurici[5], André Báfica[1,4], Matthew S. Macauley[9,10], Fernando Spiller[1,2*]

[1]Laboratory of Immunobiology, [2]Department of Pharmacology, [4]Department of Microbiology, Immunology and Parasitology, [5]Department of Clinical Medicine, Federal University of Santa Catarina (UFSC), Florianopolis, Santa Catarina, Brazil.

[3]Department of Pharmacology, School of Medicine of Ribeirao Preto, University of Sao Paulo, Ribeirao Preto, Sao Paulo, Brazil.

[6]Molecular Biology Laboratory, Institute of Biomedical Research, Marcilio Dias Naval Hospital, Navy of Brazil, Rio de Janeiro, Brazil.

[7]Tuberculosis Research Laboratory, Faculty of Medicine, Federal University of Rio de Janeiro, Rio de Janeiro, Brazil; Immunoparasitology Laboratory, Oswaldo Cruz Foundation, FIOCRUZ, Rio de Janeiro, Brazil.

[8]Department of Immunology, Paulo de Goes Institute of Microbiology, Federal University of Rio de Janeiro (UFRJ), Rio de Janeiro, Brazil.

[9]Department of Chemistry, [10]Department of Medical Microbiology and Immunology, University of Alberta, Edmonton, Alberta, Canada.

*Corresponding author: Fernando Spiller, Department of Pharmacology (FMC/CCB/UFSC), Av. Prof. Henrique da Silva Fontes, 321 - Trindade, Florianópolis – SC, 88040-900, Tel.: +55-48-3721-4852. e-mail: fernando.spiller@ufsc.br, spiller.farmaco@gmail.com.

ABSTRACT

Neutrophils overstimulation plays a crucial role in tissue damage during severe infections. Neuraminidase-mediated cleavage of surface sialic acid has been demonstrated to regulate leukocyte responses. Here, we report that antiviral neuraminidase inhibitors constrain host neuraminidase activity, surface sialic acid release, ROS production, and NETs released by microbial-activated human neutrophils. *In vivo*, treatment with Oseltamivir results in infection control and host survival in murine models of sepsis. Moreover, Oseltamivir or Zanamivir treatment of whole blood cells from severe COVID-19 patients reduces host NEU-mediated shedding of surface sialic acid and neutrophil overactivation. These findings suggest that neuraminidase inhibitors are host-directed interventions to dampen neutrophil dysfunction in severe infections.

Keywords: neuraminidase; sialic acid; sepsis; Oseltamivir; Zanamivir, neutrophil; SARS-CoV-2; COVID-19.

INTRODUCTION

Neutrophils are key components of the immune response against multiple pathogens[1]. However, during acute severe infections, such as sepsis and COVID-19, overactivated neutrophils infiltrate vital organs and release many molecules including proteases, reactive oxygen species (ROS), and neutrophil extracellular traps (NETs)[2,3]. While such inflammatory mediators are essential to the control of infection, they can also damage healthy cells[4]. Therefore, the function of neutrophils must be regulated to efficiently clear microorganisms with minimal detrimental effects to the host.

A number of mechanisms controlling neutrophil activation have been described[5]. For instance, the contents of sialic acid (Sia) have been demonstrated to regulate leukocyte activation to microbial stimuli[6,7]. The dense array of Sia present in the glycocalyx of all mammalian cells makes this monosaccharide a central molecule for many cellular processes including: cell-cell interaction, signal transduction, and transendothelial migration[8]. Neuraminidases (NEUs) are enzymes found in both pathogens and mammalian hosts[9], which hydrolyze Sia residues linked to galactose, N-acetylgalactosamine or polySia residues on glycoconjugates, thereby regulating many physiological and pathological responses[10]. In human neutrophils, shedding of surface Sia by microbial-derived NEUs leads to cellular activation, ROS production, and NETs release[7,11–13]. Additionally, it has been demonstrated that LPS induces membrane-associated NEU activation in murine or human macrophages and dendritic cells[14]. Upon LPS binding to TLR4, NEU activity was shown to regulate NF-κB induction in

71 macrophages, suggesting a role for this enzyme during cellular activation[14].
72 Furthermore, in experimental Gram-negative sepsis or endotoxemia, NEU activity
73 mediated leukocyte dysfunction, associated with exacerbated inflammatory response
74 and high mortality rates[15,16]. As previous studies have demonstrated that pathogen-
75 derived NEU stimulate neutrophils[7,11,17], we investigated whether endogenous host
76 NEUs can be targeted to regulate neutrophil dysfunction observed in severe infections.
77
78 Here, we have identified host NEU activation as a positive regulator of microbial-
79 induced human neutrophil overactivation. Additionally, we have employed the antiviral
80 NEU inhibitors Oseltamivir and Zanamivir to explore this pathway and found that these
81 drugs fine-tune the neutrophil dysfunction observed in sepsis and COVID-19. Together,
82 our results show that NEU is a potential target for the control of neutrophil dysfunction
83 and presenting Oseltamivir or Zanamivir as adjunctive therapy for severe infections.

RESULTS

LPS-induced surface Sia shedding in human neutrophils is mediated by NEU activity

As activated NEUs hydrolyze Sia residues linked to underlying galactose glycoconjugates[8], we employed a flow cytometry-based lectin binding assay to measure Sia levels on neutrophils after their activation. Alpha2-3-Sia is a major functional Sia linkage of surface glycans present on human neutrophils[18]. Therefore, we used the lectin MAL-II that binds selectively to α2-3- over α2-6-linked Sia[19]. LPS treatment of whole blood from healthy donors significantly reduces the binding of MAL-II on neutrophils ($CD66b^+$) when compared to untreated cells (**Supplementary Fig. 2A**). Next, cells were stained with Fc-chimera of Siglec-9, a sialic acid-binding protein that recognize Sia in α2-3 and α2-6 linkages[20]. Similarly, we observed that binding of Siglec-9-Fc (**Supplementary Fig. 2B**) is decreased on neutrophils treated with LPS, confirming a reduction of neutrophil Sia residues likely due to LPS-induced NEU activity in these cells. To test this hypothesis, we measured NEU activity in human leukocytes using the NEU substrate 4-MU-NANA[14] and validated the assay using NEU purified from *C. perfringens* (CpNEU) (**Fig. 1A-B)**. Both clinically available NEU inhibitors Oseltamivir and Zanamivir reduce CpNEU activity (**Fig. 1A-B)**. Using total leukocytes from healthy donors, we observed that LPS-induced NEU activity was significantly inhibited by Oseltamivir or Zanamivir (**Fig. 1C-D**). Moreover, these NEU inhibitors prevent LPS- or CpNEU-mediated reduction of MAL-II binding on neutrophils surface

(**Fig. 1E-H**). Together, these results show that LPS-induced host NEU activity decreases Sia content on neutrophils, which can be inhibited by Oseltamivir and Zanamivir.

LPS-induced phagocytosis and killing of *E. coli* is modulated by NEU activity

Bacteria uptake and killing are important functions of neutrophils[4]. We next investigated whether host NEU regulates phagocytosis and killing of *E. coli.* Whole blood or total leukocytes from healthy donors were preincubated with LPS or CpNEU, respectively, and *E. coli* BioParticles® added to cells for 60 min. Ingested pHrodo *E. coli* by neutrophils were analyzed by flow cytometry. As expected, we observed a significant increase in MFI of pHrodo *E. coli* of unstimulated cells at 37 ^{o}C when compared to cells at 4 ^{o}C (**Supplementary Fig. 3**). LPS (**Fig. 2A-C**) or CpNEU, used as a positive control (**Fig. 2D-F**), but not heat-inactivated CpNEU, significantly enhances phagocytosis of *E. coli*. Remarkably, these effects are inhibited by Zanamivir or Oseltamivir (**Fig. 2A-F**), suggesting that LPS-enhanced phagocytosis involves a host NEU-dependent pathway. Similarly, pretreatment of cells with LPS or CpNEU increases both the number of cells with bacteria as well as the number of bacteria per cell (**Fig. 2G-J**). These effects were also abolished when NEU inhibitors Oseltamivir and Zanamivir were added in the cell cultures (**Fig. 2G-J**). Furthermore, LPS or CpNEU treatment enhances intracellular and extracellular killing of *E. coli,* which are also inhibited by Oseltamivir or Zanamivir (**Fig. 2K-L**). These results suggest that NEU plays a critical role in LPS-stimulated phagocytosis and killing responses of neutrophils.

NEU blockade prevents neutrophil activation

Shedding of cell surface Sia by mobilization of granule-associated NEU to the cell surface has been associated with neutrophil activation[21]. Therefore, we analyzed surface expression of CD66b and CD62L, two markers of human neutrophil activation[22–24], and α2-3-Sia levels in LPS-exposed whole blood cultures. Both Oseltamivir and Zanamivir inhibit LPS-induced shedding of α2-3-Sia (**Fig. 3A,B**) and CD62L (**Fig. 3D,E**) or upregulation of CD66b (**Fig. 3G,H**) on neutrophils. Similarly, MAL-II preincubation, which prevents hydrolysis of α2-3-Sia by NEU[25] by steric hindrance at the NEU cleavage site, blocks LPS-induced neutrophil activation (**Fig. 3C,F,I).** These data show that dampening NEU activity or blocking the hydrolysis of α2-3-Sia is sufficient to inhibit human neutrophil activation by LPS. Similar results were observed in soluble CpNEU-treated leukocytes (**Supplementary Fig. 4**). Next, we assessed whether NEU inhibitors influenced LPS-stimulated ROS production and NETs release, key mediators of bacterial killing and tissue injury[26]. We observed that neutrophils primed with LPS and stimulated with PMA produce higher amounts of ROS when compared to unprimed cells **(Fig. 3J-L)**. Both Oseltamivir and Zanamivir inhibit ROS release to levels similar to unprimed cells. These results were also reproduced by the treatment of cells with CpNEU (**Supplementary Fig. 5E-G**). Furthermore, Oseltamivir or Zanamivir significantly inhibit LPS-induced NETs released by isolated neutrophils **(Fig. 3M)**. Together, these data indicate that microbial-induced host NEU activity regulates important neutrophil functions *in vitro*.

Oseltamivir enhances survival rate of mice in clinically relevant models of sepsis

Exacerbated neutrophil responses such as increased ROS production, NETs release, and degranulation are associated with tissue injury and organ dysfunction[27]. By using Oseltamivir as a therapeutic tool, we next explored the involvement of NEU activity *in vivo* during experimental sepsis, a model of neutrophil dysfunction[3,28,29]. We first induced sepsis by intraperitoneal administration of 1 x 10^7 CFU/mice of the Gram-negative *E. coli* (ATCC 25922), which lacks NEU in its genome[30]. We used the dose of 10 mg/Kg of Oseltamivir by oral gavage (PO), which is the equivalent dose used in humans (~7.5 mg/Kg)[31]. Oseltamivir pretreatment (2 hr before infection) plus post-treatment (6 hr after infection, 12/12 h, PO, for 4 days) markedly boost host survival (**Supplementary Fig. 6A**). Only a single dose of Oseltamivir before (2 hr) bacterial administration was sufficient to reduce disease pathology. Oseltamivir significantly decreases the number of neutrophils in the BAL and lung tissue 4 or 6 hr after infection (**Supplementary Fig. 6B-C**). This pretreatment also augments the neutrophil migration to the focus of infection, which is associated with an efficient control of infection (**Supplementary Fig. 6D-F**). Furthermore, pretreatment with Oseltamivir decreases BAL and plasma TNF and IL-17 levels (**Supplementary Fig. 6G-J**) and tissue injury markers (AST, ALT, ALP and total bilirubin) (**Supplementary Fig. 6K-N**), as well as prevents reduction of α2-3-Sia on peritoneal lavage SSC^{high}/$GR\text{-}1^{high}$ cells (**Supplementary Fig. 6O-P**). More importantly, the post-treatment efficacy of Oseltamivir was also evaluated in survival of septic mice. Mice were IP challenged with *E. coli* (1 x 10^7 CFU/mice) and treated 6 hr after infection with Oseltamivir for 4 days (10 mg/Kg, PO, 12/12h). Strikingly, in the post-treatment protocol, Oseltamivir

provides a significant improvement in the survival rate of septic mice (**Supplementary Fig. 6Q**).

Next, we employed the CLP model to evaluate the effect of Oseltamivir in septic mice, as it is considered the gold standard in preclinical sepsis[32]. Six hours after CLP, mice were treated with Oseltamivir for 4 days (10 mg/Kg, PO, 12/12h). This treatment leads to a small delay in the mortality rate of severe septic mice (**Fig. 4A**). Next, CLP septic mice were treated with antibiotics because it is one of the standard interventions used in clinical settings of sepsis[33]. Importantly, compared to the control animals, therapeutic use of Oseltamivir plus antibiotics drastically improved survival rates of CLP mice (87.5% experimental group vs 25% control group) (**Fig. 4B**). Forty-eight hr after surgery, post-treated septic mice have a significant reduction of neutrophils in BAL and lungs, improvement of neutrophil migration at the focus of infection, and reduced bacterial load in PL and blood (**Fig. 4C-G**). Levels of TNF and IL-17 in PL and plasma and tissue injury markers were also reduced in Oseltamivir treated mice (**Fig. 4H-O**). Additionally, Oseltamivir also leads to a higher expression of α2-3-Sia on SSC^{high}/$GR\text{-}1^{high}$ cells in PL (**Fig. 4P-Q**) confirming blockade of NEU activity *in vivo*.

As respiratory tract infections, particularly pneumonia, are among the most common sites of infection in sepsis[34], we intratracheally administered *K. pneumoniae* (ATCC 700603) into mice to address the effect of Oseltamivir. Post-treatment of mice with Oseltamivir significantly improves survival of septic mice challenged with *K. pneumoniae* (**Fig. 5A**). The increased host survival was accompanied by a decrease of

neutrophil migration in BAL, reduced levels of TNF and IL-17 and reduced levels of tissue injury markers (**Fig. 5B-K**). Oseltamivir also prevents reduction of α2-3-Sia on BAL SSC^{high}/GR-1^{high} cells (**Fig. 5L-M**). Together, these results show that host NEU activation exacerbates inflammatory responses during sepsis and the use of Oseltamivir improves disease outcome.

Oseltamivir and Zanamivir rescue overactivated neutrophils from COVID-19 patients

Similar to bacterial sepsis, recent evidence suggests that neutrophils fuel hyper-inflammatory response during severe SARS-CoV-2 infection. Larger numbers of circulating neutrophils have been associated with poor prognosis of COVID-19 patients and analysis of lung biopsies and autopsy specimens showed extensive neutrophil infiltration[2,35–41]. For instance, using single-cell analysis of whole blood from mild and severe COVID-19 patients, Schulte-Schrepping *et al*. (2020) showed that neutrophils in severe patients are highly activated, mainly characterized by the shedding of CD62L[42]. Confirming previous findings, we observed that neutrophils from active COVID-19 patients, but not from convalescent patients, displayed shedding of CD62L (**Fig. 6A**) and upregulation of CD66b (**Fig. 6B**), indicating a high activation state of these cells. Moreover, neutrophils from severe COVID-19 patients were found to present a significant reduction of surface α2-3-Sia (**Fig. 6C)**, suggesting that NEU activity is increased during severe COVID-19. Therefore, we ask whether neuraminidase inhibitors can rescue neutrophil activation from COVID-19 patients. *Ex vivo* treatment of

whole blood with Oseltamivir or Zanamivir decreased neutrophil activation and restored the levels of cell surface α2-3-Sia (**Fig. 6D-F**). **Fig. 6G** summarizes the effects of Oseltamivir and Zanamivir on the surface levels of CD62L and α2-3-Sia by neutrophils, where these treatments lead to a formation of two different clusters in cells from severe COVID-19 patients. As soluble NEU enzymes are also present in plasma[15], we next asked if plasma from COVID-19 patients can induce neutrophil response from healthy donors. Indeed, stimulation of whole blood from healthy donors with fresh plasma from severe, but not convalescent, COVID-19 patients leads to neutrophil activation (**Fig. 6H**), reduction of α2-3-Sia (**Fig. 6I**) as well as ROS production (**Fig. 6J,K**), which were significantly reduced by Oseltamivir or Zanamivir (**Fig. 6H-J**). Additionally, we observed that activity of NEU is increased in plasma from severe COVID-19 patients (**Supplementary Fig. 7A)**. Serum glycoproteins from severe COVID-19 patients also presented reduced levels of α2-3-Sia (**Supplementary Fig. 7B-E**) suggesting NEU activation *in vivo*. Moreover, plasma samples from severe COVID-19 patients that were heat-inactivated to inhibit soluble NEU activity **(Supplementary Fig. 7F**) still induces neutrophil activation, suggesting that cellular NEU in conjunction with circulating factors mediate NEU-dependent neutrophil activation in severe COVID-19. These results highlight host NEU as a regulator of neutrophil activation in severe COVID-19 and suggest this pathway as a potential host-directed intervention target to rewire neutrophil responses during severe disease.

DISCUSSION

Systemic inflammatory response may lead to unsuitable neutrophil stimulation, which is associated with higher mortality rates in sepsis and sepsis-like diseases[43]. Therefore, finding new therapeutic options to prevent neutrophil overstimulation while maintaining their microbicidal abilities is hugely desired. Neuraminidase inhibitors are promising drugs to fill this gap. Here we demonstrated that endogenous host NEUs mediate exacerbated inflammatory responses by primary neutrophils. Clinically used viral NEU inhibitors, Oseltamivir and Zanamivir, decrease human NEU activity and are effective in prevent LPS-induced neutrophil responses or to rescue overactivation of neutrophils from COVID-19 patients. In severe murine sepsis, therapeutic use of Oseltamivir fine-tunes neutrophil migration results in bacterial clearance and high survival rates.

All of the four different isotypes of NEU described in mammals (NEU1, NEU2, NEU3 and NEU4) remove Sia from glycoproteins and glycolipids with specific substrate preferences[44]. NEU1 cleaves preferentially α2-3-Sia and seems to be the most important isoenzyme in immune cells. NEU1 is a lysosomal enzyme but it is also present at the cell surface where it can regulate multiple receptors such as Fc gamma receptor (FcγR), insulin receptor, integrin β-4, and TLRs[45]. While several stimuli were described to induce NEU activity including LPS[14], PMA, calcium ionophore A23187, fMLP[21], and IL-8[46], how NEUs are activated is poorly understood. However, NEU1 activation involves formation of a multicomplex of enzymes that stabilizes NEU1 in its conformational active state[47]. Interestingly, NEU1 was found to be associated with

matrix metalloproteinase-9 (MMP9) at the surface of naive macrophages[48]. LPS binding to TLR4 leads to activation of a G protein-coupled receptor (GPCR) via Gαi subunit and MMP9 to induce NEU1 activity, which in turn removes α2-3-Sia from TLR4, allowing its dimerization and intracellular signaling[25,48,49]. Although we have not formally addressed whether the LPS-TLR4 pathway directly activates NEU function in human neutrophils, our results employing MAL-II preincubation suggest desialylation is required for LPS-mediated neutrophil responses. Thus, it is possible that NEU controls Sia levels in TLR4 molecules in human neutrophils as observed in macrophages and dendritic cells[25,49]. The effects of LPS on neutrophil responses observed here are in accordance with the well-documented induction of ROS and NETs as well as in phagocytosis and bacterial killing by these phagocytes[50–54]. Importantly, the upstream involvement of NEU regulating LPS responses by neutrophils is in agreement with the previous demonstration that TLRs stimulate these cells independent of gene transcription[50]. Together, our data suggests that NEU activation provides a fast response to enhance microbial-induced neutrophil functions. Thus, we speculate that this could be an evolutionary mechanism by which neutrophils quickly mobilize their microbicidal mediators against pathogens.

Sialic acid removal from neutrophils surface markedly changes their adhesiveness, chemotaxis, and migration[21,55–58]. In peritonitis- or pneumonia-induced sepsis in mice, we observed that Oseltamivir prevented the massive neutrophil infiltration into bronchoalveolar spaces or lung tissues, suggesting that regulation of neutrophil migration by dampening NEU activity contributes to survival of septic mice. Interestingly,

we observed a divergent effect of Oseltamivir on neutrophil migration to the focus of infection between peritonitis- and pneumonia-induced sepsis. This could be explained by the different mechanisms involved in neutrophil migration to the peritoneal cavity and lungs. While expression of CD62L and rolling of neutrophils to endothelium is necessary for its migration to the peritoneal cavity, it seems to be not required for migration into the lungs[3,59]. Moreover, systemic neutrophil activation leads to cell stiffening, resulting in retention of neutrophils in the small capillaries of the lungs[60], which is frequently the first organ impaired in non-pneumonia- and pneumonia-induced sepsis[61]. The role of NEU-induced neutrophil activation suggested here is in agreement with previous demonstration that NEU1 deletion in hematopoietic cells confers resistance to endotoxemia[16]. Also, the sialidase inhibitor Neu5Gc2en protects endotoxemic irradiated wild-type (WT) mice reconstituted with WT bone marrow but not WT mice reconstituted with NEU1$^{-/-}$ bone marrow cells[16]. Similar to our finds, the treatment of mice with NEU inhibitors increases host survival in *E. coli*-induced sepsis[15]. This outcome was correlated with significant inhibition of blood NEU activity. Enhancement of soluble NEU activity in serum decreases the Sia residues from alkaline phosphatase (APL) enzymes, which are involved in the clearance of circulating LPS-phosphate during sepsis[15].

SARS-CoV-2 infection leads to mild illness in most of the patients, but ~20% of them progress to severe disease with many characteristics resembling sepsis, including acute respiratory distress syndrome (ARDS), cytokine storm, and neutrophil dysregulation[38,62–64]. The transcriptional programs found in neutrophil subsets from blood and lungs of severe, but not mild, COVID-19 patients are related to cell dysfunction, coagulation, and

NETs formation[39,42]. We observed that blood neutrophils from severe COVID-19 are highly activated as demonstrated by reduced CD62L expression and increase of CD66b expression, as previously reported[42]. We now add new information by showing that neutrophils from severe, but not convalescent, COVID-19 patients have reduced surface levels of α2-3-Sia, suggesting a relevant role of NEU for neutrophil activation during COVID-19. More importantly, both the NEU inhibitors Oseltamivir and Zanamivir, increased the α2-3-Sia content and rewired the overactivation of neutrophils from severe COVID-19 patients. We speculate that the addition of NEUs competitive inhibitors allowed the endogenous sialyltransferases to restore sialyl residues on surface glycoconjugates. Fast changes of surface sialic acid levels by sialidases and sialyltransferases seems to be an important mechanism to control neutrophil response[55]. In neutrophils from healthy donors or COVID-19 convalescent patients, Oseltamivir and Zanamivir did not interfere in resting state and had no effect on α2-3-Sia content, suggesting that NEU has a low effect on surface Sia turnover on non-activated neutrophils. How neutrophils are activated and the role of NEU in this process remains to be defined in COVID-19, nevertheless, recent evidence showed that neutrophils could be directly activated by SARS-CoV-2[2], cytokines[65], and alarmins[39,42] such as calprotectin[39], a TLR4 ligand[66]. In addition, we now add new evidence by showing that soluble NEU together with other circulating factors present in plasma from severe COVID-19 patients also accounts for neutrophil activation.

Collectively, this work suggests that host NEU activation leads to shedding of surface sialic acid with consequent neutrophil overstimulation, tissue damage, and high

mortality rates. On the other hand, NEU inhibitors-prevented shedding of sialic acid and regulates neutrophil response, resulting in infection control and high survival rates (working model in **Supplementary Fig. 8**). Taking into account that both drugs are broadly used in humans with well-known toxic and adverse effects, our data suggest Oseltamivir and Zanamivir could be repurposed for the treatment of sepsis or severe infections such as COVID-19. Interestingly, a retrospective single-center cohort study including 1190 patients with COVID-19 in Wuhan, China, showed that administration of Oseltamivir was associated with a decreased risk of death in severe patients[67]. Our data suggest that such encouraging results may be explained by the inhibition of NEU-mediated neutrophil dysfunction *in vivo*. Nevertheless, randomized clinical trials with clinically used NEU inhibitors in sepsis and COVID-19 are required to directly explore this hypothesis.

MATERIALS AND METHODS

Human blood samples

Blood was collected from healthy donors (25 - 45 yr old, n=3-12) in endotoxin-free tubes with K_3EDTA (Labor Import, Brasil). All participants gave their written informed consent for blood collection after been informed on procedures. The research protocol followed the World Medical Association Declaration of Helsinki and was approved by the Institutional Review Board of the Federal University of Santa Catarina (CAAE #82815718.2.0000.0121). Blood samples were also collected from severe COVID-19 (n=6) or convalescent COVID-19 (n=8) patients (25 to 89 yr old) admitted in the Intensive Care Unit (ICU) or NUPAIVA (Research Center on Asthma and Airway Inflammation) at the UFSC University Hospital from August to October 2020. Blood samples from sex-matched healthy donors were used as controls. All patients or a close family member gave consent for participation in the study, which was approved by the UFSC IRB (CAAE #36944620.5.1001.0121). Supplementary Table 1 summarizes patients clinical and laboratory records. These samples were used to analyze neutrophil activation, surface α2-3-Sia as well as the effect of plasma under these parameters and ROS production. Blood samples were also collected from severe COVID-19 (n=5) patients (55 to 73 yr old) admitted at the Hospital Naval Marcílio Dias (HNMD). The research was approved by the Research Ethics Committee (CEP) from Brazilian National Health Council. All patients signed a free and informed consent form following current legislation and the relevant ethical regulations approved by the Hospital Naval Marcílio Dias (CAAE #31642720.5.0000.5256). These samples were used to analyze

the sialylation of plasma proteins. Supplementary Table 2 summarizes the clinical and laboratory information of patients from this cohort.

Evaluation of neutrophil activation, phagocytosis, killing, ROS, and NETs release

Whole blood containing 1 x 10^6 leukocytes were incubated (37 ^oC, 5% CO_2) in the presence or absence of Oseltamivir (100 µM, Sigma-Aldrich, San Luis, MO, USA), Zanamivir (30 µM, Sigma-Aldrich), LPS (1 µg/mL, *E. coli* 0127:b8, Sigma-Aldrich), LPS plus Oseltamivir or LPS plus Zanamivir for 90 min. Concentrations of Oseltamivir and Zanamivir used here were chosen by concentration-effect experiments (10-100 µM Oseltavimir and 1-30 µM Zanamivir) (data not shown). Since plasma is a rich source of glycoconjugates, total leukocytes were used instead of whole blood to evaluate the effect of isolated neuraminidase from *Clostridium perfringens* (CpNEU) on neutrophils. Red blood cells (RBCs) were lysed by lysis buffer (0.15 M NH_4Cl; 0.1 mM EDTA; 12 mM Na_2HCO_3) for 7 min, RT, followed by centrifugation (270 x g; 22°C; 7 min). Total leukocytes (1 x 10^6 cells) were incubated (37 ^oC, 5% CO_2) in the presence or absence of CpNEU (10 mU, Sigma-Aldrich), CpNEU plus Oseltamivir (100 µM) or CpNEU plus Zanamivir (30 µM) for 60 min. Next, the following assays were performed. *Analysis of neutrophil activation*. Leukocytes were then washed and resuspended in FACS buffer (2 mM EDTA/PBS). The mix of antibodies against CD66b (G10F5; BioLegend, San Diego, CA, USA), CD62L (DREG-56; BioLegend), CD16 (3G8; BioLegend), isotypes or *Maackia amurensis* Lectin II biotinylated (MAL-II, Vector Labs, San Diego, CA, USA) coupled to Streptavidin (Biolegend), plus human BD Fc Block™ (BD Pharmingen™) and Fixable Viability Stain (FVS, BD Horizon™, San Jose, CA, USA) were added to

leukocytes for 30 min at 4 °C. Cells were washed, resuspended in FACS buffer, acquired in a FACSVerse cytometer and analyzed using FlowJo software (FlowJo LLC). Approximately 100.000 gated events were acquired in each analysis. *Phagocytosis assays*. After RBCs lysis, 1 x 10^6 leukocytes were incubated at 37 °C (5% CO_2) or at 4 °C (control) with 100 µg/mL pHrodo™ Red *E. coli* BioParticles® (Thermo Fisher, Waltham, MA, USA) for 60 min and the MFI of neutrophils ($FVS^-/CD66b^+$ cells) with ingested bioparticle was analyzed by FACS. Total leukocytes were also incubated with 1 x 10^6 CFU of live *E. coli* (ATCC 25922) for 90 min (37 °C, 5% CO_2). Next, the cells were washed twice (2 mM EDTA/PBS), fixed (FACS buffer/PFA 2%) and the percentage of neutrophils with bacteria or the percentage of neutrophils with ≥3 bacteria was analyzed by light microscopy using Differential Quick Stain Kit (Laborclin, Brazil). *Bacterial killing*. Total leukocytes (1 x 10^6) were incubated (37 °C, 5% CO_2) with 1 x 10^6 CFU of live *E. coli* for 180 min. The samples were centrifuged (270 g, 7 min, 4 °C) and 10 µL of supernatant were diluted until 10^6 and spread onto agar brain-heart infusion (BHI, Kasvi, Brazil) to quantify the viable extracellular bacteria. The pellets were washed twice with PBS/2 mM EDTA (270 g, 7 min, 4 °C), the leukocytes were lysed with 2% Triton-X, washed (PBS, 2000 g, 15 min, 4 °C), resuspended in PBS and 10 µL of samples were diluted until 10^6 and spread onto agar BHI. Plates were incubated overnight at 37 °C and viable bacteria were expressed as mean ± SEM of CFU/mL. *ROS assay*. After RBCs lysis, 1 x 10^6 leukocytes were incubated at 37 °C (5% CO_2) with 10 µM of cell-permeant 2',7'-dichlorodihydrofluorescein diacetate (CM-H2DCFDA, ThermoFisher) for 5 min. Next, cells were stimulated or not with phorbol 12-myristate 13-acetate (PMA) for 10 min, fixed, washed twice with PBS/2 mM EDTA (270 g, 7 min,

4 °C) and analyzed by FACS. *NETs assay*. NETs quantification was performed as previous described[68] on the supernatant of isolated neutrophils. Briefly, an anti-MPO antibody bound to a 96-well flat-bottom plate captured the enzyme MPO (5 µg/ml; Abcam), and the amount of DNA bound to the enzyme was quantified using the Quant-iT™ PicoGreen® kit (Invitrogen, Carlsbad, CA, USA) according to the manufacturer's instructions. Fluorescence intensity (Ex 488 nm/Em 525 nm) was quantified in a FlexStation 3 Microplate Reader (Molecular Devices, San Jose, CA, USA). *Neutrophil isolation*. Human circulating neutrophils were isolated by Percoll density gradients[69]. Briefly, four different gradients, 72%, 65%, 54%, and 45%, were used to isolate human circulating neutrophils. After centrifugation at 600 g for 30 min at 4 °C, the cell layer at the 72% gradient interface was collected as the neutrophil fraction. The erythrocytes were removed by lysis, and cell pellets were resuspended in RPMI 1640. Isolated neutrophils (1 x 10^6/well) were treated with Oseltamivir, Zanamivir or medium 1 h before the stimulus with PMA (50 nM) or LPS (10 µg/mL). After 4 hr of stimuli (37 °C, 5% CO_2), the supernatant was collected to measure the levels of NETs.

Neutrophil responses with plasma from COVID-19 patients

Whole blood samples from sex-matched healthy donors (n = 7) were incubated for 2 h (37 °C, 5% CO_2) with 7% of fresh plasma from healthy donors, severe or convalescent COVID-19 patients or heat-inactivated plasma (56 °C, 30 min) from severe COVID-19 patients in the presence or absence of Oseltamivir (100 µM) or Zanamivir (30 µM). Surface levels of α2-3-Sia and CD66b and ROS production were assessed on neutrophils by FACS.

438

439 **Neuraminidase kinetics assay**

440 After RBCs lysis, 0.5 x 10^6 leukocytes were resuspended in HBSS and added to 96-well
441 flat-bottom dark plate (SPL Life Sciences, South Korea) on ice. Then, 4-
442 Methylumbelliferyl-N-acetyl-α-D-Neuramic Acid (4-MU-NANA, Sigma-Aldrich) substrate
443 (0.025 mM) was added followed by medium, or LPS (1 µg/mL), LPS plus Oseltamivir
444 (100 µM), LPS plus Zanamivir (30 µM). CpNEU (10 mU), CpNEU plus Oseltamivir or
445 CpNEU plus Zanamivir were used as positive controls of the assay. The volume was
446 completed to 200 µL with HBSS, followed by reading on the Spectramax® Paradigm®
447 instrument starting 3 min after and every 5 min for 55 min at 37 ºC. Sialidase activity
448 was also assessed in heat-inactivated or fresh plasma from severe COVID-19 patients
449 in the presence or absence of Oseltamivir (100 µM) or Zanamivir (30 µM) using Tecan
450 Infinite 200 multi-reader. The fluorescent substrate 4-MU-NANA formation was detected
451 at ex 350 nm/em 450 nm.

452

453 **Mice**

454 The care and treatment of the animals were based on the Guide for the Care and Use
455 of Laboratory Animals[70] and all procedures followed the ARRIVE guidelines and the
456 international principles for laboratory animal studies[71]. C57BL/6 (Jackson Laboratory,
457 Bar Harbor, ME, USA) mice (8–10 weeks old) and Swiss mice (10–12 weeks old) were
458 housed in cages at 21 ± 2°C with free access to water and food at the Animal Facility of
459 the Department of Microbiology, Immunology, and Parasitology and Department of
460 Pharmacology from UFSC, respectively. A total of 228 mice were used in this study.

Protocols were approved by the Animal Use Ethics Committee of UFSC (CEUA #8278290818).

E. coli-, Klebsiella pneumoniae- and CLP-induced sepsis

E. coli (ATCC 25922, Manassas, VA, USA) or *K. pneumoniae* (ATCC 700603) were used to induce severe sepsis in mice. Naive mice were intraperitoneal (IP) challenged with 100 µL of 1 x 10^7 CFU of the *E. coli* suspension. A group of *E. coli*-septic mice was randomly pretreated (2 hr before infection) and post treated by *per oral* (PO, 12/12 hr) via with saline or Oseltamivir phosphate (10 mg/kg, Eurofarma, Brazil) for 4 days to survival analysis. Another group was pretreated 2 hr before infection with a single dose of Oseltamivir phosphate (10 mg/kg, PO) and the pathophysiological response was analyzed at 4 and 6 hr after infection. *E. coli*-septic mice were also randomly posttreated (6 hr after infection, 12/12 hr) with saline or Oseltamivir phosphate (PO, 10 mg/kg) for 4 days to survival analysis. For pneumonia-induced sepsis, mice were anesthetized with isoflurane (3–5 vol%) and placed in supine position. A small incision was made in the neck where the trachea could be localized and a *K. pneumoniae* suspension (4 x 10^8 CFU/50 µL of PBS) was injected into the trachea with a sterile 30-gauge needle. Skin was sutured and animals were left for recovery in a warm cage. After 6 hr of infection and then 12/12 hr mice were treated with Oseltamivir phosphate (PO, 10 mg/kg) for survival analysis. In another set of experiments, pneumonia was induced and mice were treated 6 hr after infection with a single dose of Oseltamivir phosphate (10 mg/kg, PO) for material collection and analysis of pathophysiological response 24 hr after infection.

Cecal ligation and puncture (CLP)-induced sepsis were performed as previously described[28]. Mice were anesthetized with xylazine (2 mg/kg, IP, Syntec, Brazil) followed by isoflurane (3–5 vol%, BioChimico, Brazil), a 1 cm midline incision was made in the anterior abdomen, and the cecum was exposed and ligated below the ileocecal junction. The cecum was punctured twice with an 18-gauge needle and gently squeezed to allow its contents to be released through the punctures. Sham-operated (Sham) animals underwent identical laparotomy but without cecal ligation and puncture. The cecum was repositioned in the abdomen, and the peritoneal wall was closed. All animals received 1 mL of 0.9% saline subcutaneous (SC) and 100 µL of tramadol (5 mg/kg, SC, Vitalis, Brazil) immediately after CLP. CLP-septic mice were randomly treated (starting 6 h after infection, PO) with 100 µL of saline or Oseltamivir phosphate (10 mg/kg, 12/12 hr) for 4 days. In another set of experiments, CLP mice were randomly IP treated (6 hr after infection, 12/12 hr) during 4 days with 100 µL metronidazole (15 mg/kg, Isofarma, Brazil) plus ceftriaxone (40 mg/kg, Eurofarma, Brazil) and Oseltamivir phosphate (10 mg/kg) or saline by PO to survival analysis or treated for 36 hr to analyze the pathophysiological response at 48 hr after CLP.

Neutrophil migration

The animals were euthanized in a CO_2 chamber, the bronchoalveolar lavage (BAL) and peritoneal lavage (PL) were performed and the number of neutrophils was determined at 4 and 6 hr after *E. coli*, 24 hr after *K. pneumoniae* infection or 48 hr after CLP surgery, as described[28]. Next, mice were perfused with PBS/EDTA (1 mM) and the lungs were harvested. Lungs were passed through 40-µm nylon cell strainers and

single-cell suspensions were centrifuged in 35% Percoll® solution (315 mOsm/kg, Sigma-Aldrich) for 15 min at 700 g to enrich leukocytes populations. Pelleted cells were then collected, and erythrocytes were lysed. Single-cell suspensions from individual mice were determined using a cell counter (Coulter ACT, Beckman Coulter, Brea, CA, USA) or with a haemocytometer. Differential counts were also determined on Cytospin smears stained using Differential Quick Stain Kit (Laborclin, Brazil). Blood samples were collected by heart puncture and tubes containing heparin for further analysis. Neutrophils from LP or BAL were also stained with anti-Ly-6G/Ly-6C (GR-1, RB6-8C5; BioLegend) and MAL-II to be further analyzed by FACS, as previously described. Analysis was carried out in $SSC^{high}/GR\text{-}1^{high}$ cells.

Bacterial counts

The bacterial counts were determined as previously described[28]. Briefly, the BAL, PL or blood were harvested and 10 µL of samples were plated on Muller-Hinton agar dishes (Difco Laboratories, Waltham, MA, USA) and incubated for 24 hr at 37 °C. PL or BAL samples were diluted until 10^6.

ELISA

TNF (R&D Systems, Minneapolis, MN, USA) and IL-17 (XpressBio Life Sciences Products, Frederick, MD, USA) levels in plasma, PL or BAL were determined by ELISA kits according to the manufacturer's instructions.

Tissue injury biochemical markers

Aspartate aminotransferase (AST), alanine aminotransferase (ALT), alkaline phosphatase (ALP) activities, and the levels of total bilirubin were determined in plasma samples by commercial kits (Labtest Diagnóstica, Brazil). The procedures were carried out according to the manufacturer's instructions.

Lectin blotting of serum glycoproteins

To evaluate if severe COVID-19 changes the α2-3 sialylation of serum glycoproteins, serum samples from four healthy donors and five severe COVID-19 patients were blotted with MAL-II as previously described[72]. Samples were diluted in SDS-PAGE sample buffer and heated at 100 °C for 5 min. Twelve µg of total protein were resolved in 10% SDS-PAGE and transferred onto nitrocellulose membranes (Millipore, Burlington, MA, USA). Membranes were blocked (TBST + 5% BSA) overnight at 4 ^{o}C and incubated for 2 hr with 1 µg/mL of biotin-conjugated MAL-II, washed and incubated for 40 min with alkaline-phosphatase (ALP)-conjugated streptavidin (Southern Biotec, Birmingham, AL, USA) diluted 1:10.000. Both MAL-II and streptavidin-ALP were diluted in TBST (5% BSA plus 150 mM of $CaCl_2$). Membranes were then revealed with BCIP/NBT (5-bromo-4-chloro-3-indolyl-phosphate/nitro blue tetrazolium) color development substrate (Promega, Brazil). The lane intensities were quantified using the Image J software. In parallel, the resolved SDS-PAGE were stained with Coomassie Brilliant blue R 250 (Merck KGaA, Germany) to compare the protein profile between the different samples.

Statistical analysis

The data are reported as the mean or median ± SEM of the values obtained from two to seven independent experiments. Each experiment using human samples was performed using three to five samples from healthy donors or one to three samples from severe or convalescent COVID-19 patients. We used five mice per experimental group except for survival analyses in which twelve to twenty mice were used. The mean or median values for the different groups were compared by analysis of variance (ANOVA) followed by Dunnett and/or Tukey post-tests. Bacterial counts were analyzed by the Mann–Whitney *U*-test or unpaired *t*-test using a parametric test with Welch's correction. Survival curves were plotted using the Kaplan–Meier method and then compared using the log-rank method and Gehan-Wilcoxon test. Data was analyzed using GraphPad Prism version 8.00 for Mac (GraphPad Software, USA). A $P < 0.05$ was considered significant.

Abbreviations

4-MU-NANA 4-methylumbelliferyl-N-acetyl-α -D-Neuramic Acid

ALP alkaline phosphatase

ALT alanine aminotransferase

ARRIVE Animal Research: Reporting of In Vivo Experiments

AST aspartate aminotransferase

ATCC American Type Culture Collection

BAL bronchoalveolar lavage

BHI brain–heart infusion

CD cluster of differentiation

CFU colony forming units

CLP cecal ligation and puncture

CM-H2DCFDA cell-permeant 2',7'-dichlorodihydrofluorescein diacetate

CpNEU *Clostridium perfringens* neuraminidase

DANA 2,3-dehydro-2-deoxy-N-acetylneuraminic acid

EDTA ethylenediamine tetra-acetic acid

FACS fluorescence-activated cell sorting

578 FcγR Fc gamma receptor

579 fMLP N-formyl-Met-Leu-Phe

580 FVS fixable viability stain

581 HBSS Hanks' balanced salt solution

582 IgG immunoglobulin G

583 IP intraperitoneal pathway

584 LPS lipopolysaccharide

585 MAL-II *Maackia amurensis* lectin II

586 MFI median fluorescence intensity

587 NETs neutrophil extracellular traps

588 NEU neuraminidases

589 Neu5Ac2en 2-deoxy-2, 3-didehydro-D-N-acetylneuraminic acid

590 PBS phosphate buffered saline

591 PFA paraformaldehyde

592 PL peritoneal lavage

593 PMA 12-myristate 13-acetate

594 PMN polymorphonuclear

595 PO oral pathway

596 RBCs red blood cells

597 ROS reactive oxygen species

598 SARS-CoV-2 severe acute respiratory syndrome coronavirus 2

599 SC subcutaneous pathway

600 Sia sialic acids

601 Siglecs sialic acid-binding immunoglobulin-like lectins

602 TLR toll-like receptor

603 COVID-19 coronavirus disease 2019

604 WT wild-type

Acknowledgments

We thank UFSC microscopy (LCME) and biology (LAMEB) facilities for technical support.

Authors' contributions

All named authors meet the criteria for authorship of this manuscript, take responsibility for the work's integrity as a whole, and have given final approval for publication.

ROF, FCA, DM, RS, DSM, AB, MSM and FS designed experiments and analyzed data; ROF, FAC, CFS, DM, CWW, CLB, AAS, JA, LFF, CCN, NMP, PCS, FRF, FAS, LA, NH, AB and FS performed experiments; SB, AM, MSM, FQC and RM contributed with critical reagents/tools/clinical samples; ROF, FS, AB wrote the manuscript.

Competing Interests statement

The authors declare that no conflict of interest exists.

Funding

This work was funded by FAPESP-SCRIPPS (FS; 15/50387-4), Howard Hughes Medical Institute – Early Career Scientist (AB; 55007412), National Institutes of Health Global Research Initiative Program (AB; TW008276), CAPES Computational Biology (DSM; 23038.010048/2013–27), CNPQ/COVID-19 (AB; 401209/2020-2), CNPQ/PQ Scholars (AB and DSM), FAPESC Scholarship (DM).

627 **REFERENCES**

628 1. Mócsai, A. Diverse novel functions of neutrophils in immunity, inflammation, and beyond. *J.*
629 *Exp. Med.* **210**, 1283–1299 (2013).
630 2. Veras, F. P. *et al.* SARS-CoV-2-triggered neutrophil extracellular traps mediate COVID-19
631 pathology. *J. Exp. Med.* **217**, (2020).
632 3. Alves-Filho, J. C., Spiller, F. & Cunha, F. Q. Neutrophil paralysis in sepsis. *Shock* **34 Suppl**
633 **1**, 15–21 (2010).
634 4. Segal, A. W. How neutrophils kill microbes. *Annu. Rev. Immunol.* **23**, 197–223 (2005).
635 5. Steevels, T. A. M. & Meyaard, L. Immune inhibitory receptors: essential regulators of
636 phagocyte function. *Eur. J. Immunol.* **41**, 575–587 (2011).
637 6. Macauley, M. S., Crocker, P. R. & Paulson, J. C. Siglec-mediated regulation of immune cell
638 function in disease. *Nat. Rev. Immunol.* **14**, 653–666 (2014).
639 7. Chang, Y.-C., Uchiyama, S., Varki, A. & Nizet, V. Leukocyte inflammatory responses
640 provoked by pneumococcal sialidase. *MBio* **3**, (2012).
641 8. Varki, A. Sialic acids in human health and disease. *Trends. Mol. Med.* **14,** 351–360 (2008).
642 9. Lipničanová, S., Chmelová, D., Ondrejovič, M., Frecer, V. & Miertuš, S. Diversity of
643 sialidases found in the human body - A review. *Int. J. Biol. Macromol.* **148**, 857–868 (2020).
644 10. Varki, A. & Gagneux, P. Multifarious roles of sialic acids in immunity. *Ann. N. Y. Acad. Sci.*
645 **1253**, 16–36 (2012).
646 11. Suzuki, H., Kurita, T. & Kakinuma, K. Effects of neuraminidase on O2 consumption and
647 release of O2 and H2O2 from phagocytosing human polymorphonuclear leukocytes. *Blood*
648 **60,** 446–453 (1982).
649 12. Arora, D. J. S. & Henrichon, M. Superoxide Anion Production in Influenza Protein-Activated
650 NADPH Oxidase of Human Polymorphonuclear Leukocytes. *J. Infect. Dis.* **169**, 1129–1133
651 (1994).

13. Henricks, P. A., van Erne-van der Tol, M. E. & Verhoef, J. Partial removal of sialic acid enhances phagocytosis and the generation of superoxide and chemiluminescence by polymorphonuclear leukocytes. *J. Immunol.* **129**, 745–750 (1982).
14. Amith, S. R. *et al.* Dependence of pathogen molecule-induced Toll-like receptor activation and cell function on Neu1 sialidase. *Glycoconj. J.* **26**, 1197–1212 (2009).
15. Yang, W. H. *et al.* Accelerated Aging and Clearance of Host Anti-inflammatory Enzymes by Discrete Pathogens Fuels Sepsis. *Cell. Host. Microbe.* **24**, 500–513.e5 (2018).
16. Chen, G.-Y. *et al.* Broad and direct interaction between TLR and Siglec families of pattern recognition receptors and its regulation by Neu1. *Elife* **3**, e04066 (2014).
17. Mills, E. L., Debets-Ossenkopp, Y., Verbrugh, H. A. & Verhoef, J. Initiation of the respiratory burst of human neutrophils by influenza virus. *Infect. Immun.* **32**, 1200–1205 (1981).
18. Mondal, N. *et al.* ST3Gal-4 is the primary sialyltransferase regulating the synthesis of E-, P- , and L-selectin ligands on human myeloid leukocytes. *Blood* **125,** 687–696 (2015).
19. Knibbs, R. N., Goldstein, I. J., Ratcliffe, R. M. & Shibuya, N. Characterization of the carbohydrate binding specificity of the leukoagglutinating lectin from Maackia amurensis. Comparison with other sialic acid-specific lectins. *J. Biol. Chem.* **266**, 83–88 (1991).
20. Movsisyan, L. D. & Macauley, M. S. Structural advances of Siglecs: insight into synthetic glycan ligands for immunomodulation. *Org. Biomol. Chem.* **18**, 5784–5797 (2020).
21. Cross, A. S. & Wright, D. G. Mobilization of sialidase from intracellular stores to the surface of human neutrophils and its role in stimulated adhesion responses of these cells. *J. Clin. Invest.* **88**, 2067–2076 (1991).
22. Schmidt, T. *et al.* CD66b overexpression and homotypic aggregation of human peripheral blood neutrophils after activation by a gram-positive stimulus. *J. Leukoc. Biol.* **91**, 791–802 (2012).
23. Kishimoto, T. K., Jutila, M. A., Berg, E. L. & Butcher, E. C. Neutrophil Mac-1 and MEL-14 adhesion proteins inversely regulated by chemotactic factors. *Science* **245**, 1238–1241

(1989).

24. Jutila, M. A., Rott, L., Berg, E. L. & Butcher, E. C. Function and regulation of the neutrophil MEL-14 antigen in vivo: comparison with LFA-1 and MAC-1. *J. Immunol.* **143**, 3318–3324 (1989).

25. Amith, S. R. *et al.* Neu1 desialylation of sialyl alpha-2,3-linked beta-galactosyl residues of TOLL-like receptor 4 is essential for receptor activation and cellular signaling. *Cell. Signal.* **22**, 314–324 (2010).

26. Mittal, M., Siddiqui, M. R., Tran, K., Reddy, S. P. & Malik, A. B. Reactive oxygen species in inflammation and tissue injury. *Antioxid. Redox Signal.* **20**, 1126–1167 (2014).

27. Sônego, F. *et al.* Paradoxical Roles of the Neutrophil in Sepsis: Protective and Deleterious. *Front. Immunol.* **7**, 155 (2016).

28. Spiller, F. *et al.* Hydrogen Sulfide Improves Neutrophil Migration and Survival in Sepsis via K ATPChannel Activation. *Am. J. Respir. Crit. Care Med.* **182**, 360–368 (2010).

29. Spiller, F. *et al.* 1-Acid Glycoprotein Decreases Neutrophil Migration and Increases Susceptibility to Sepsis in Diabetic Mice. *Diabetes* **61**, 1584–1591 (2012).

30. Vimr, E. R. & Troy, F. A. Identification of an inducible catabolic system for sialic acids (nan) in Escherichia coli. *J. Bacteriol.* **164**, 845–853 (1985).

31. Butler, C. C. *et al.* Oseltamivir plus usual care versus usual care for influenza-like illness in primary care: an open-label, pragmatic, randomised controlled trial. *Lancet* **395**, 42–52 (2020).

32. Rittirsch, D., Huber-Lang, M. S., Flierl, M. A. & Ward, P. A. Immunodesign of experimental sepsis by cecal ligation and puncture. *Nat. Protoc.* **4**, 31–36 (2009).

33. Rhodes, A. *et al.* Surviving Sepsis Campaign: International Guidelines for Management of Sepsis and Septic Shock: 2016. *Crit. Care Med.* **45**, 486–552 (2017).

34. Chou, E. H. *et al.* Incidence, trends, and outcomes of infection sites among hospitalizations of sepsis: A nationwide study. *PLoS One* **15**, e0227752 (2020).

704 35. Middleton, E. A. *et al.* Neutrophil extracellular traps contribute to immunothrombosis in
705 COVID-19 acute respiratory distress syndrome. *Blood* **136**, 1169–1179 (2020).
706 36. Schurink, B. *et al.* Viral presence and immunopathology in patients with lethal COVID-19: a
707 prospective autopsy cohort study. *Lancet Microbe*. **7**, e290-e299 (2020).
708 37. Huang, C. *et al.* Clinical features of patients infected with 2019 novel coronavirus in Wuhan,
709 China. *Lancet* **395**, 497–506 (2020).
710 38. Guan, W.-J. *et al.* Clinical Characteristics of Coronavirus Disease 2019 in China. *N. Engl. J.*
711 *Med.* **382**, 1708–1720 (2020).
712 39. Silvin, A. *et al.* Elevated Calprotectin and Abnormal Myeloid Cell Subsets Discriminate
713 Severe from Mild COVID-19. *Cell* **182**, 1401–1418.e18 (2020).
714 40. Wilk, A. J. *et al.* A single-cell atlas of the peripheral immune response in patients with
715 severe COVID-19. *Nat. Med.* **26**, 1070–1076 (2020).
716 41. Kuri-Cervantes, L. *et al.* Comprehensive mapping of immune perturbations associated with
717 severe COVID-19. *Sci Immunol* **5**, (2020).
718 42. Schulte-Schrepping, J. *et al.* Severe COVID-19 Is Marked by a Dysregulated Myeloid Cell
719 Compartment. *Cell* **182**, 1419–1440.e23 (2020).
720 43. Leliefeld, P. H. C., Wessels, C. M., Leenen, L. P. H., Koenderman, L. & Pillay, J. The role of
721 neutrophils in immune dysfunction during severe inflammation. *Crit. Care* **20**, 73 (2016).
722 44. Smutova, V. *et al.* Structural basis for substrate specificity of mammalian neuraminidases.
723 *PLoS One* **9**, e106320 (2014).
724 45. Glanz, V. Y., Myasoedova, V. A., Grechko, A. V. & Orekhov, A. N. Sialidase activity in
725 human pathologies. *Eur. J. Pharmacol.* **842**, 345–350 (2019).
726 46. Cross, A. S. *et al.* Recruitment of murine neutrophils in vivo through endogenous sialidase
727 activity. *J. Biol. Chem.* **278**, 4112–4120 (2003).
728 47. Pshezhetsky, A. V. & Hinek, A. Where catabolism meets signalling: neuraminidase 1 as a
729 modulator of cell receptors. *Glycoconj. J.* **28**, 441–452 (2011).

730 48. Abdulkhalek, S. *et al.* Neu1 sialidase and matrix metalloproteinase-9 cross-talk is essential
731 for Toll-like receptor activation and cellular signaling. *J. Biol. Chem.* **286**, 36532–36549
732 (2011).
733 49. Feng, C. *et al.* Sialyl residues modulate LPS-mediated signaling through the Toll-like
734 receptor 4 complex. *PLoS One* **7**, e32359 (2012).
735 50. Blander, J. M. & Medzhitov, R. Regulation of phagosome maturation by signals from toll-
736 like receptors. *Science* **304**, 1014–1018 (2004).
737 51. Doyle, S. E. *et al.* Toll-like receptors induce a phagocytic gene program through p38. *J.*
738 *Exp. Med.* **199**, 81–90 (2004).
739 52. El-Benna, J., Dang, P. M.-C. & Gougerot-Pocidalo, M.-A. Priming of the neutrophil NADPH
740 oxidase activation: role of p47phox phosphorylation and NOX2 mobilization to the plasma
741 membrane. *Semin. Immunopathol.* **30**, 279–289 (2008).
742 53. Brinkmann, V. Neutrophil Extracellular Traps Kill Bacteria. *Science* **303**, 1532–1535 (2004).
743 54. Böhmer, R. H., Trinkle, L. S. & Staneck, J. L. Dose effects of LPS on neutrophils- in a
744 whole blood flow cytometric assay of phagocytosis and oxidative burst. *Cytometry* **13**, 525–
745 531 (1992).
746 55. Rifat, S. *et al.* Expression of sialyltransferase activity on intact human neutrophils. *J.*
747 *Leukoc. Biol.* **84**, 1075–1081 (2008).
748 56. Cross, A. S. *et al.* Recruitment of Murine Neutrophils in Vivo through Endogenous Sialidase
749 Activity. *J. Biol. Chem.* **278**, 4112–4120 (2003).
750 57. Feng, C. *et al.* Endogenous PMN sialidase activity exposes activation epitope on
751 CD11b/CD18 which enhances its binding interaction with ICAM-1. *J. Leukoc. Biol.* **90**, 313–
752 321 (2011).
753 58. Sakarya, S. *et al.* Mobilization of neutrophil sialidase activity desialylates the pulmonary
754 vascular endothelial surface and increases resting neutrophil adhesion to and migration
755 across the endothelium. *Glycobiology* **14**, 481–494 (2004).

59. Petri, B., Phillipson, M. & Kubes, P. The Physiology of Leukocyte Recruitment: An In Vivo Perspective. *J. Immunol.* **180**, 6439–6446 (2008).

60. Worthen, G., Schwab, B., Elson, E. & Downey, G. Mechanics of stimulated neutrophils: cell stiffening induces retention in capillaries. *Science* **245**, 183–186 (1989).

61. Sheu, C.-C. *et al.* Clinical characteristics and outcomes of sepsis-related vs non-sepsis-related ARDS. *Chest* **138**, 559–567 (2010).

62. Wang, T. *et al.* Comorbidities and multi-organ injuries in the treatment of COVID-19. *Lancet* **395**, e52 (2020).

63. Wu, Z. & McGoogan, J. M. Characteristics of and Important Lessons From the Coronavirus Disease 2019 (COVID-19) Outbreak in China: Summary of a Report of 72 314 Cases From the Chinese Center for Disease Control and Prevention. *JAMA* **323**, 1239–1242 (2020).

64. Hottz, E. D. *et al.* Platelet activation and platelet-monocyte aggregate formation trigger tissue factor expression in patients with severe COVID-19. *Blood* **136**, 1330–1341 (2020).

65. Wang, J., Jiang, M., Chen, X. & Montaner, L. J. Cytokine storm and leukocyte changes in mild versus severe SARS- CoV- 2 infection: Review of 3939 COVID- 19 patients in China and emerging pathogenesis and therapy concepts. *J. Leukoc. Biol.* **108**, 17–41 (2020).

66. Vogl, T. *et al.* Autoinhibitory regulation of S100A8/S100A9 alarmin activity locally restricts sterile inflammation. *J. Clin. Invest.* **128**, 1852–1866 (2018).

67. Liu, J. *et al.* Clinical outcomes of COVID-19 in Wuhan, China: a large cohort study. *Ann. Intensive Care* **10**, 99 (2020).

68. Czaikoski, P. G. *et al.* Neutrophil Extracellular Traps Induce Organ Damage during Experimental and Clinical Sepsis. *PLoS One* **11**, e0148142 (2016).

69. Mestriner, F. L. A. C. *et al.* Acute-phase protein alpha-1-acid glycoprotein mediates neutrophil migration failure in sepsis by a nitric oxide-dependent mechanism. *Proc. Natl. Acad. Sci. U. S. A.* **104**, 19595–19600 (2007).

70. National Research Council, Division on Earth and Life Studies, Institute for Laboratory

Animal Research & Committee for the Update of the Guide for the Care and Use of Laboratory Animals. *Guide for the Care and Use of Laboratory Animals: Eighth Edition*. (National Academies Press, 2011).

71. Kilkenny, C., Browne, W. J., Cuthill, I. C., Emerson, M. & Altman, D. G. Improving bioscience research reporting: the ARRIVE guidelines for reporting animal research. *PLoS Biol.* **8**, e1000412 (2010).

72. Xu, J. *et al.* A fixation method for the optimisation of western blotting. *Sci. Rep.* **9**, 6649 (2019).

Figures and Figure Legends

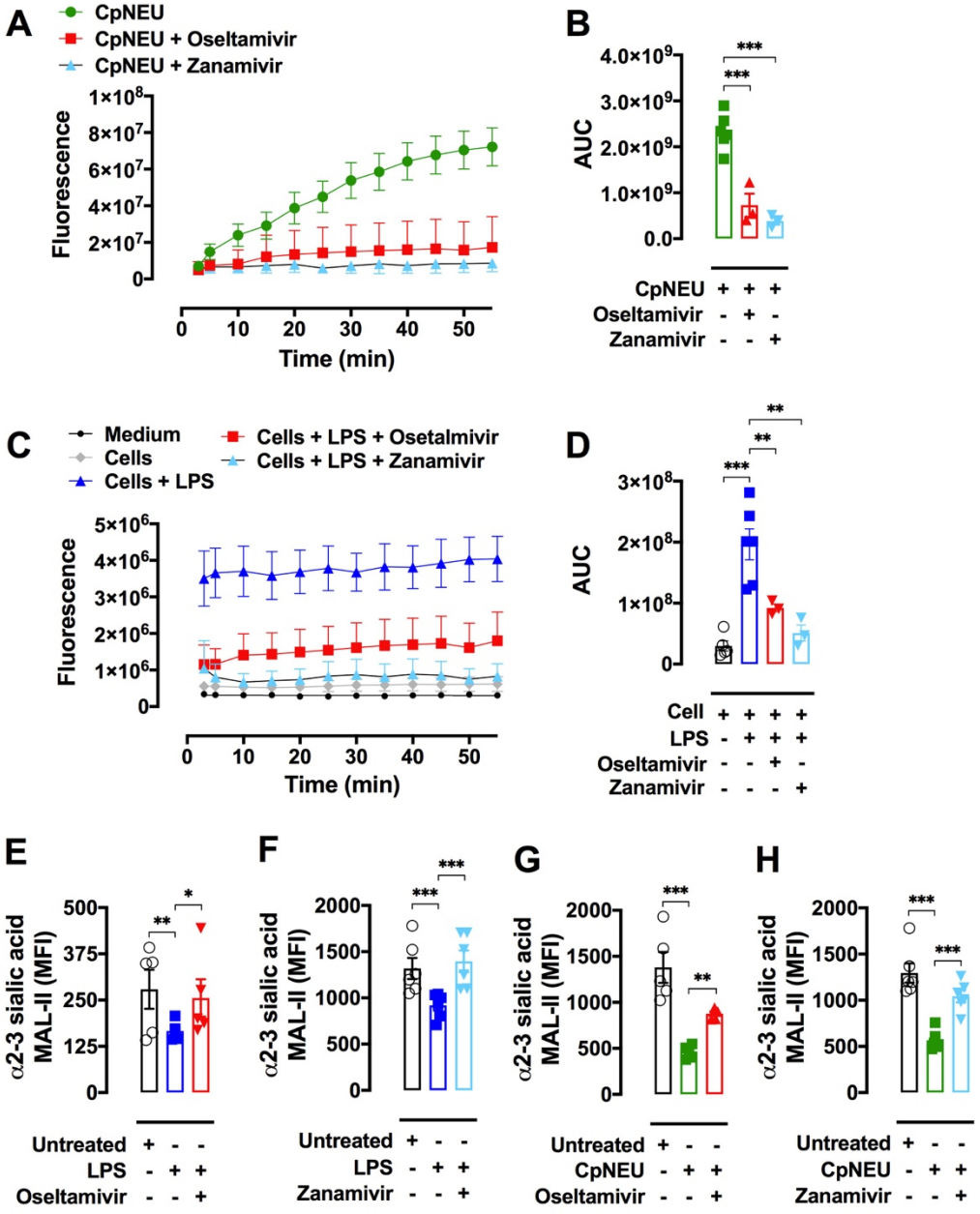

Figure 1. LPS stimulates NEU activity in human leukocytes. Neuraminidase isolated from *Clostridium perfringens* (CpNEU) was used to validate the NEU activity assay. CpNEU (0.012 UI) was added in a 96-well flat-bottom dark plate on ice in the presence or not of its inhibitors Oseltamivir phosphate (100 µM) or Zanamivir (30 µM). Next, the substrate 4-MU-NANA (0.025 mM) was added and the fluorescent substrate was read 3 min after at 37 ºC (**A**). The area under the curve (AUC) values are shown in **B**. Total

leukocytes resuspended in HBSS were added in a plate on ice and 4-MU-NANA substrate (0.025 mM) was added followed by the addition of medium, LPS (1 µg/mL), LPS plus Oseltamivir (100 µM) or LPS plus Zanamivir (30 µM). The fluorescent substrate was read 3 min after at 37 ºC (**C**). Raw data were subtracted from the control group containing only HBSS (medium) and expressed as AUC values (**D**). Whole blood containing 1 x 10^6 leukocytes from healthy donors were stimulated or not with LPS (1 µg/mL, 90 min, 37 ^{o}C, 5% CO_2), LPS plus Oseltamivir (100 µM), or LPS plus Zanamivir (30 µM). Total leukocytes (1 x 10^6) were incubated with CpNEU (10 mU, 60 min, 37 ^{o}C, 5% CO_2), CpNEU plus Oseltamivir (100 µM), or CpNEU plus Zanamivir (30 µM). Leukocytes were stained with MAL-II to detect α2-3 sialic acids (**E-F**). The MFI was analyzed on $CD66b^+$ cells using the gate strategies shown in Supplementary Fig. 1. **P* < 0.05; ***P* < 0.01; ****P* < 0.001. This figure is representative of three independent experiments (n= 3-6) and data are shown as mean ± SEM. LPS = lipopolysaccharide; MAL-II = *Maackia amurensis* lectin II; CpNEU = neuraminidase.

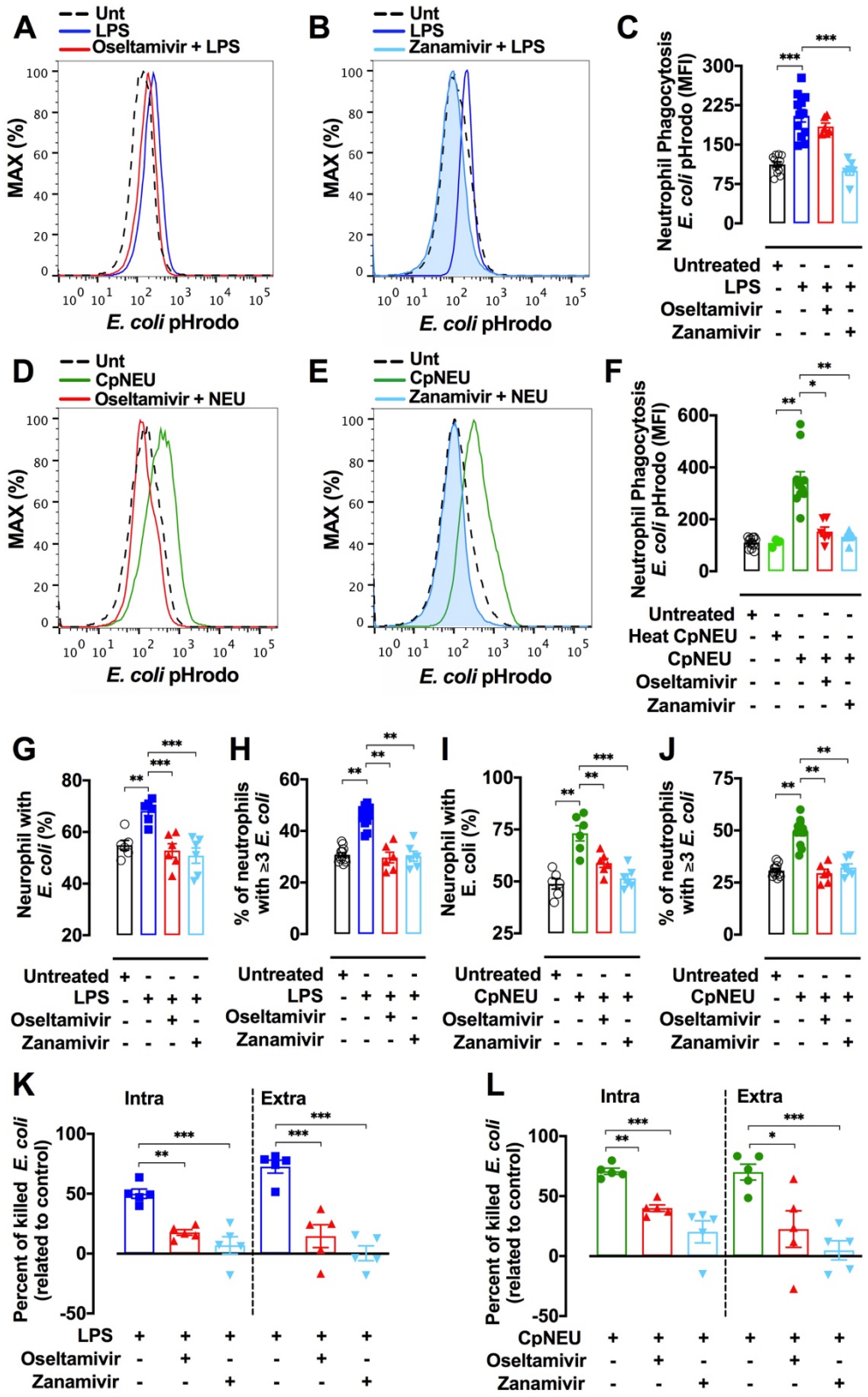

Figure 2. LPS increases phagocytosis and killing of *E. coli* in a NEU-dependent manner. Whole blood from healthy donors containing 1 x 10^6 leukocytes were exposed

(37 °C, 5% CO_2) or not to LPS (1 µg/mL, 90 min), LPS plus Oseltamivir (100 µM), or LPS plus Zanamivir (30 µM) (**A-C; G-H; K**). Total leukocytes (1 x 10^6) were exposed or not to CpNEU (10 mU, 60 min, 37 °C, 5% CO_2), CpNEU plus Oseltamivir (100 µM), or CpNEU plus Zanamivir (30 µM) (**D-F; I-J; L**) and the phagocytosis and killing assays were performed. Leukocytes were incubated with *E. coli* pHrodo BioParticles® (100 µg/mL) for 60 min at 37 °C to assess phagocytosis in viable $CD66b^+$ cells (**A-F**) (as gated in Supplementary Fig. 1). Live *E. coli* was used to evaluate phagocytosis by light microscopy or to assess the killing by leukocytes. Cells were stimulated as described above and 1 x10^6 leukocytes were incubated at 37 °C with *E. coli* (1 x10^6 CFU) for 90 min for phagocytosis or for 180 min for killing assays. The percentage of cells with ingested bacteria (**G; I**) and the number of bacterial particles per cell (**H; J**, ≥3 particles per cell) were evaluated. The killing of *E. coli* was evaluated by spreading 10 µL of supernatant (extracellular killing) or 10 µL of the intracellular content in agar medium and the CFU were counted. Killing *E. coli* was expressed as the rate of fold change compared to the unprimed (untreated) cells (**L**). Symbols represent individual donors and data are shown as mean ± SEM from pooled data of two to three independent experiments (n = 3-12). **P* < 0.05; ***P* < 0.01; ****P* < 0.001. Unt = untreated; LPS = lipopolysaccharide; CpNEU = neuraminidase.

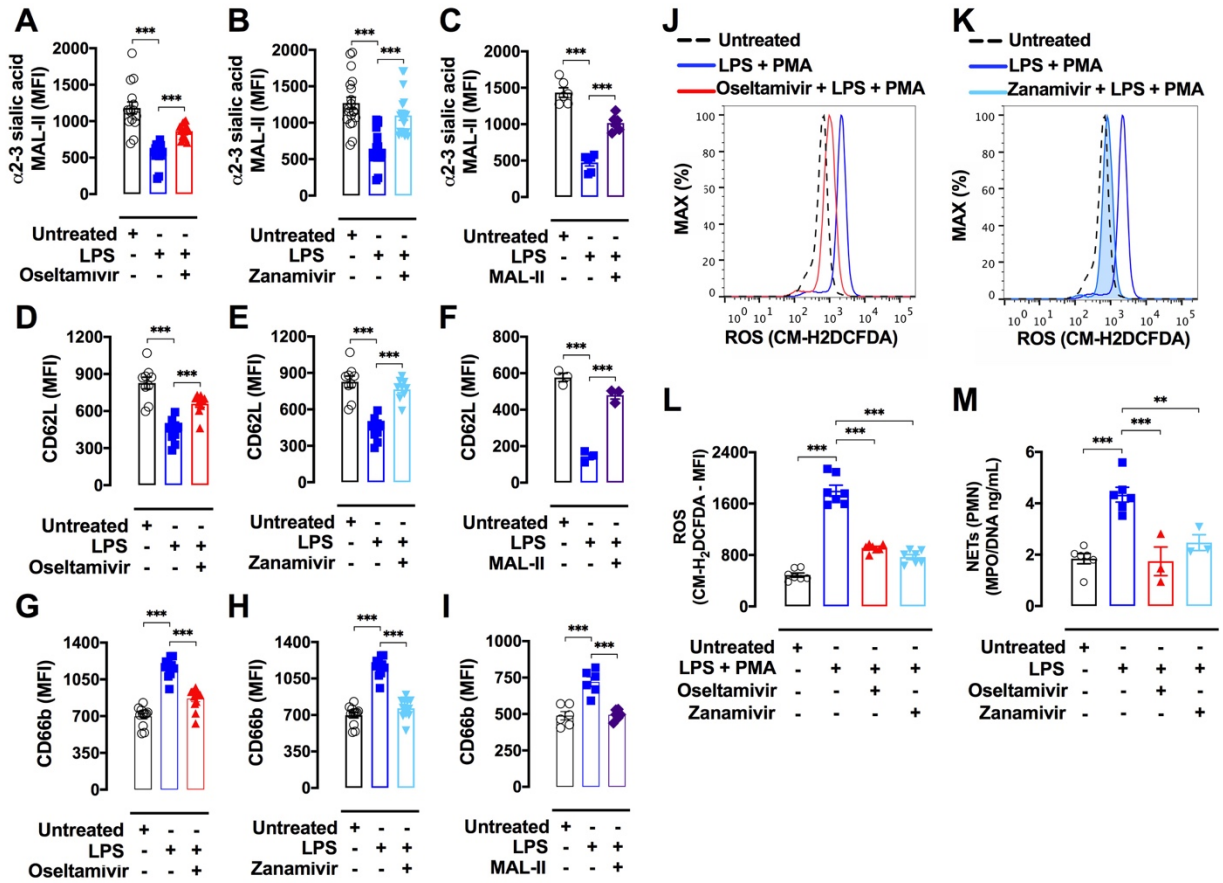

Figure 3. LPS-induced human neutrophil response involves NEU activity. Whole blood from healthy donors containing 1 x 10^6 leukocytes were stimulated or not with LPS (1 µg/mL, 90 min, 37 °C, 5% CO_2), LPS plus Oseltamivir (100 µM), LPS plus Zanamivir (30 µM), or LPS plus MAL-II (1 µg/mL, MAL-II promotes steric hindrance at the NEU cleavage site and prevent sialic acid cleavage). Leukocytes were marked with MAL-II to detect α2-3 sialic acids (**A-C**) or stained with the cell activation markers CD62L (**D-F**) and CD66b (**G-I**). After RBCs lysis leukocytes were incubated with 5 µM CM-H2DCFDA fluorescent probe for 15 min. PMA (10 µM) was used to stimulate ROS production for 10 min (**J-L**). Supplementary Fig. 5 showed ROS production in additional control groups. The MFI was analyzed on $CD66b^+$ cells using the gate strategies shown in Supplementary Fig. 1. Isolated neutrophils were treated with Osetamivir (100 µM) or Zanamivir (30 µM) 1 h before the stimulus with LPS (10 µg/mL) for 4 h. The concentration of NETs was evaluated by MPO-DNA PicoGreen assay on supernatants

of cells (**M**). Symbols represent individual donors and data are shown as mean ± SEM from pooled data of two to three independent experiments (n = 7) except for F and M that was made once with n=3. ***$P < 0.001$; **$P < 0.01$. Unt = untreated; CM-H2DCFDA = 5-(and-6)-chloromethyl-2',7'-dichlorodihydrofluorescein diacetate, acetyl ester; LPS = lipopolysaccharide; PMA = phorbol 12-myristate 13-acetate; ROS = reactive oxygen species; NETs = neutrophil extracellular traps; RBCs = red blood cells; MAL-II = *Maackia amurensis* lectin II; PMN = polymorphonuclear leukocytes.

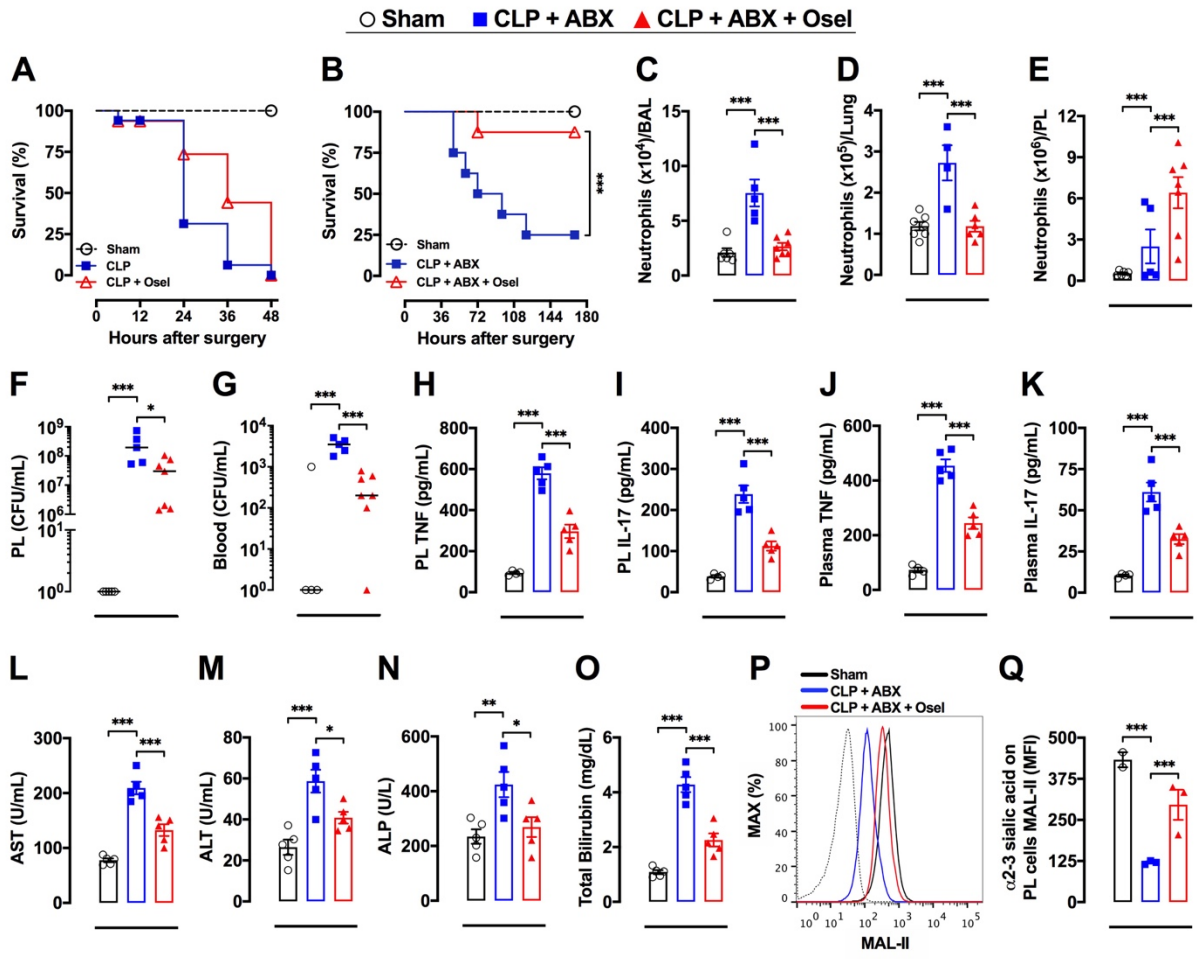

Figure 4. Oseltamivir enhanced host survival in CLP-induced sepsis. Severe sepsis was induced by the cecal ligation and puncture (CLP) model. Mice were randomly treated (starting 6 hr after infection, 12/12 h, PO, for 36 hr, n=16) with saline or Oseltamivir phosphate (10 mg/kg) and their survival rates were monitored over 48 hr (**A**). In another set of experiments, CLP mice were randomly IP treated (started 6 hr after infection, 12/12 hr) during 4 days with 100 µL metronidazole (15 mg/kg)/ceftriaxone (40 mg/kg) (ABX) plus saline or Oseltamivir phosphate (10 mg/kg) by PO and their survival rates (n=12) were monitored over 168 hr (**B**). Also, mice were subjected to CLP and treated with ABX + saline or ABX + Olsetamivir as described in B and euthanized 48 hr after surgery to evaluate the number of neutrophils in BAL (**C**), lung tissue (**D**), and peritoneal lavage (PL) (**E**); TNF (**H**), IL-17 (**I**), and CFU (**F**) were also determined in PL. Blood CFU (**G**) and plasmatic levels of TNF (**J**), IL-17 (**K**), AST (**L**), ALT (**M**), ALP (**N**) and total bilirubin (**O**) were also evaluated 48 hr after surgery.

The amount of surface α2-3 sialic acids were assessed by MAL-II staining in $SSC^{high}/Gr\text{-}1^{high}$ cells in PL and analyzed by FACS, as shown by the representative histograms (**P**) and MFI (**Q**); dotted line = unstained cells. The results are expressed as percent of survival (n=16), mean or median (only for FACS data) ± SEM. **P* < 0.05; ****P* < 0.001. These experiments were repeated 3 times for survival analysis and twice for other parameters (n=3-7). ABX = antibiotics (metronidazole/ceftriaxone); Sham = sham-operated. Osel = Oseltamivir; AST = alanine aminotransferase; ALT = aspartate aminotransferase; ALP = alkaline phosphatase; CFU = colony-forming units.

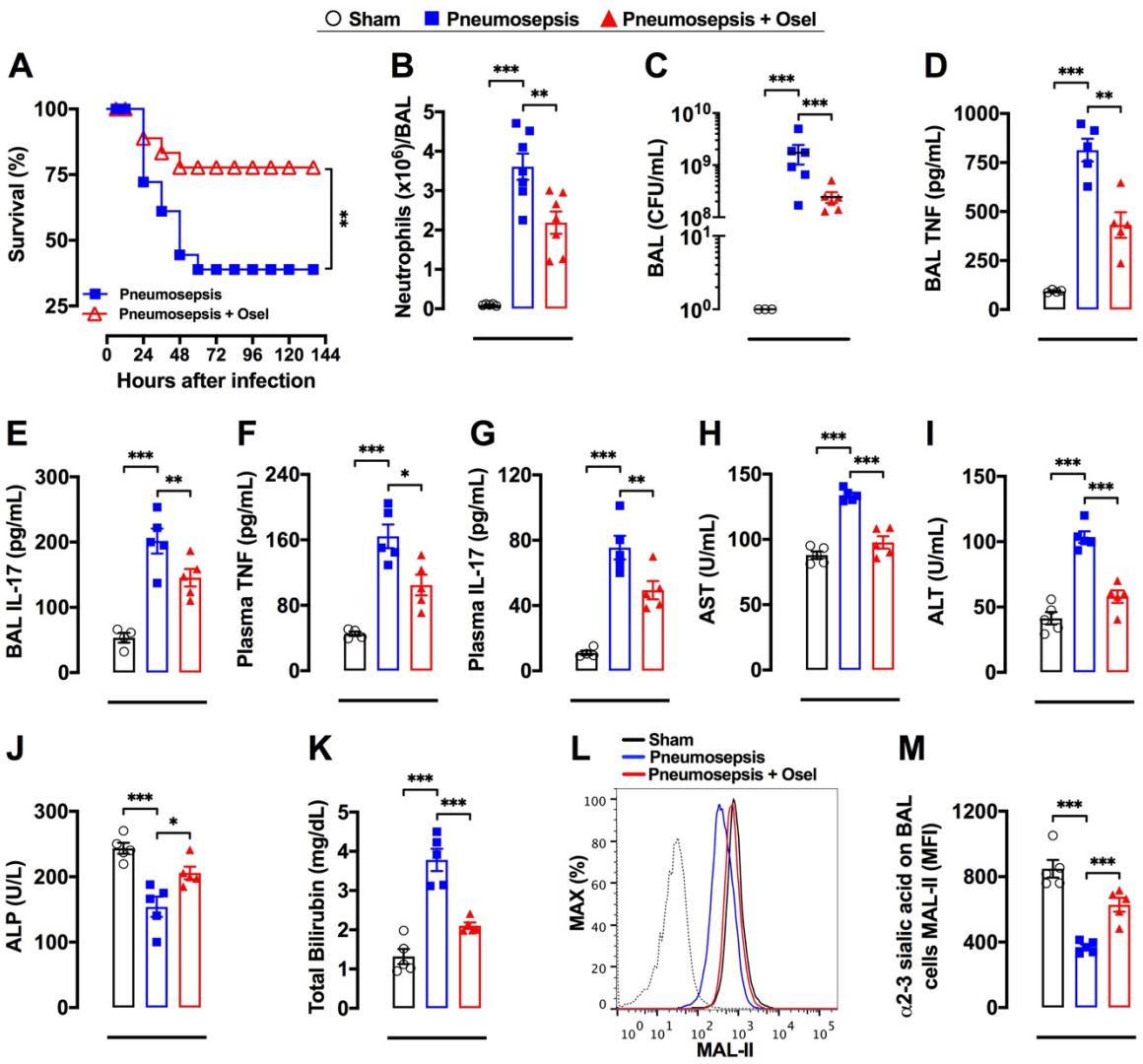

Figure 5. Oseltamivir enhanced mice survival in *K. pneumoniae*-induced sepsis. Sepsis was induced by intratracheal administration of *K. pneumoniae* and mice were randomly treated (starting 6 hr after infection, 12/12 hr, PO, n=20) with saline or Oseltamivir phosphate (10 mg/kg) and survival rates were monitored for 144 hr (**A**). In similar set of experiments, septic mice (n=6-7) were treated 6 hr after infection with a single dose of Oseltamivir phosphate (10 mg/kg, PO) and mice were euthanized 24 hr after infection to determine the number of neutrophils (**B**) and CFUs (**C**), and levels of TNF (**D**) and IL-17 (**E**) in BAL. Plasma levels of TNF (**F**), IL-17 (**G**), AST (**H**), ALT (**I**), ALP (**J**) and total bilirubin (**K**) were also evaluated 24 hr after infection. The amount of surface α2-3 sialic acids were assessed by MAL-II staining in SSC^{high}/$Gr\text{-}1^{high}$ cells in BAL and analyzed by FACS, as shown by the representative histograms (**L**) and MFI

(**M**); dotted line = unstained cells. The results are expressed as percent of survival, mean or median (only for FACS data) ± SEM. **P* < 0.05; **P* < 0.01; ****P* < 0.001. Sham = sham-operated mice; Osel = Oseltamivir; AST = alanine aminotransferase; ALT = aspartate aminotransferase; ALP = alkaline phosphatase.

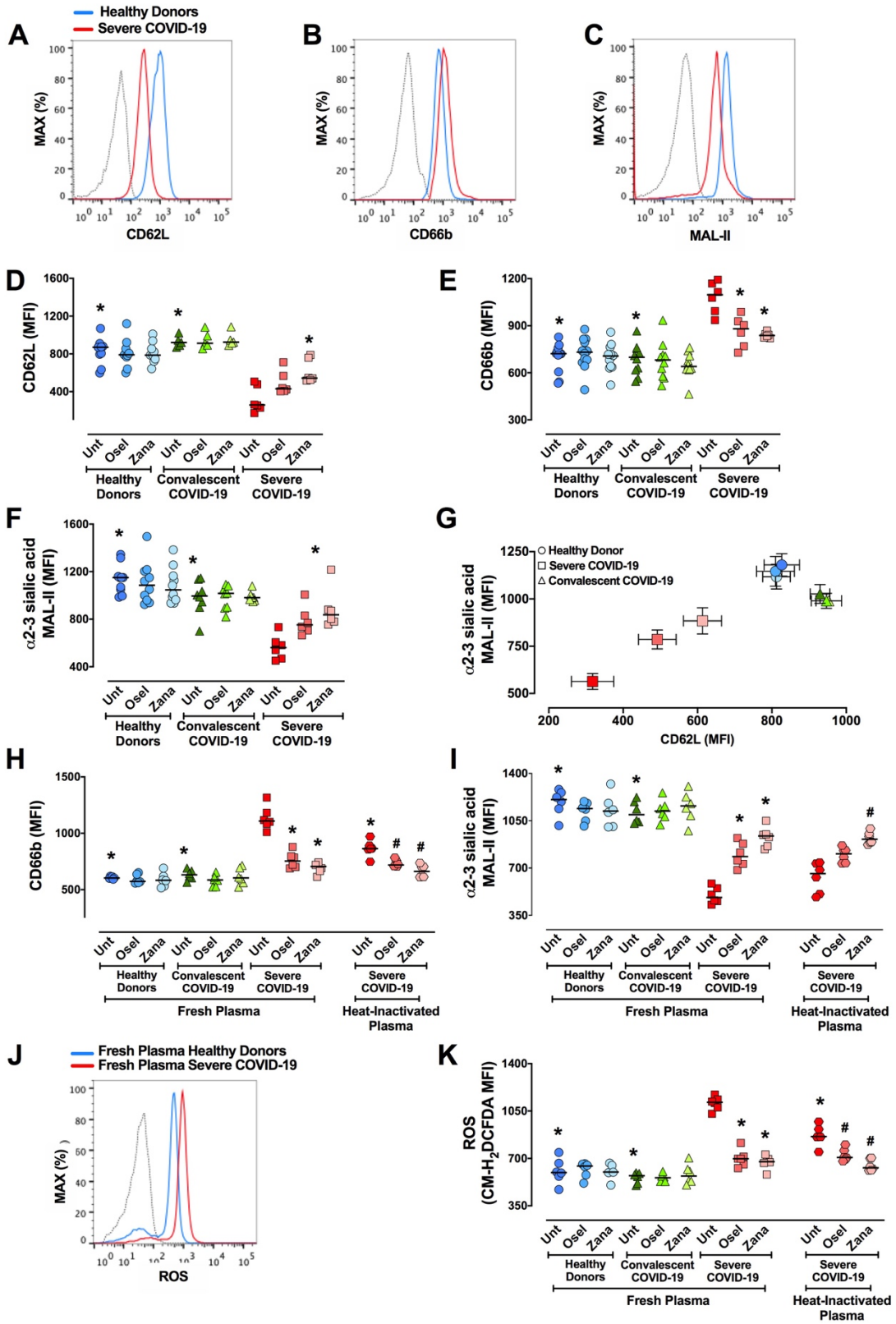

Figure 6. Oseltamivir and Zanamivir decrease neutrophil activation and increase α2-3 sialic acid levels in active, but not convalescent neutrophils from COVID-19

patients. Whole blood from healthy donors (n= 10), severe COVID-19 patients (n= 6) and convalescent COVID-19 patients (n= 8) were treated or not with Oseltamivir (100 μM) or Zanamivir (30 μM) and total leukocytes were stained with the cell activation markers CD62L (**A and D**), CD66b (**B and E**) and MAL-II to detect α2-3 sialic acids (**C and F**). Correlation of surface levels of α2-3 sialic acids vs CD62L (**G**). Blood samples from healthy donors (n = 7) were incubated for 2 h (37 °C, 5% CO_2) with 7% of fresh plasma from healthy donors, severe or convalescent COVID-19 patients or with 7% of heat-inactivated plasma from severe COVID-19 patients in the presence or absence of Oseltamivir (100 μM) or Zanamivir (30 μM) and levels of CD66b (**H**), surface α2-3-Sia (MAL-II) (**I**), and ROS production (**J, K**) were assessed by FACS. The MFI was analyzed on $CD66b^+$ cells using the gate strategies shown in Supplementary Fig. 1. Symbols represent individual donors and data are shown as scatter dot plot with line at median from pooled data of two to seven independent experiments. The statistical significance between the groups was assessed by ANOVA followed by a multiple comparisons test of Tukey. The accepted level of significance for the test was $P<0.05$. * was significantly different when compared with Untreated Severe COVID-19; # was significantly different when compared with Untreated Heat-Inactivated Plasma from Severe COVID-19. Osel = Oseltamivir; Zana = Zanamivir.

Supplementary Data

Supplementary Figures and Figure Legends

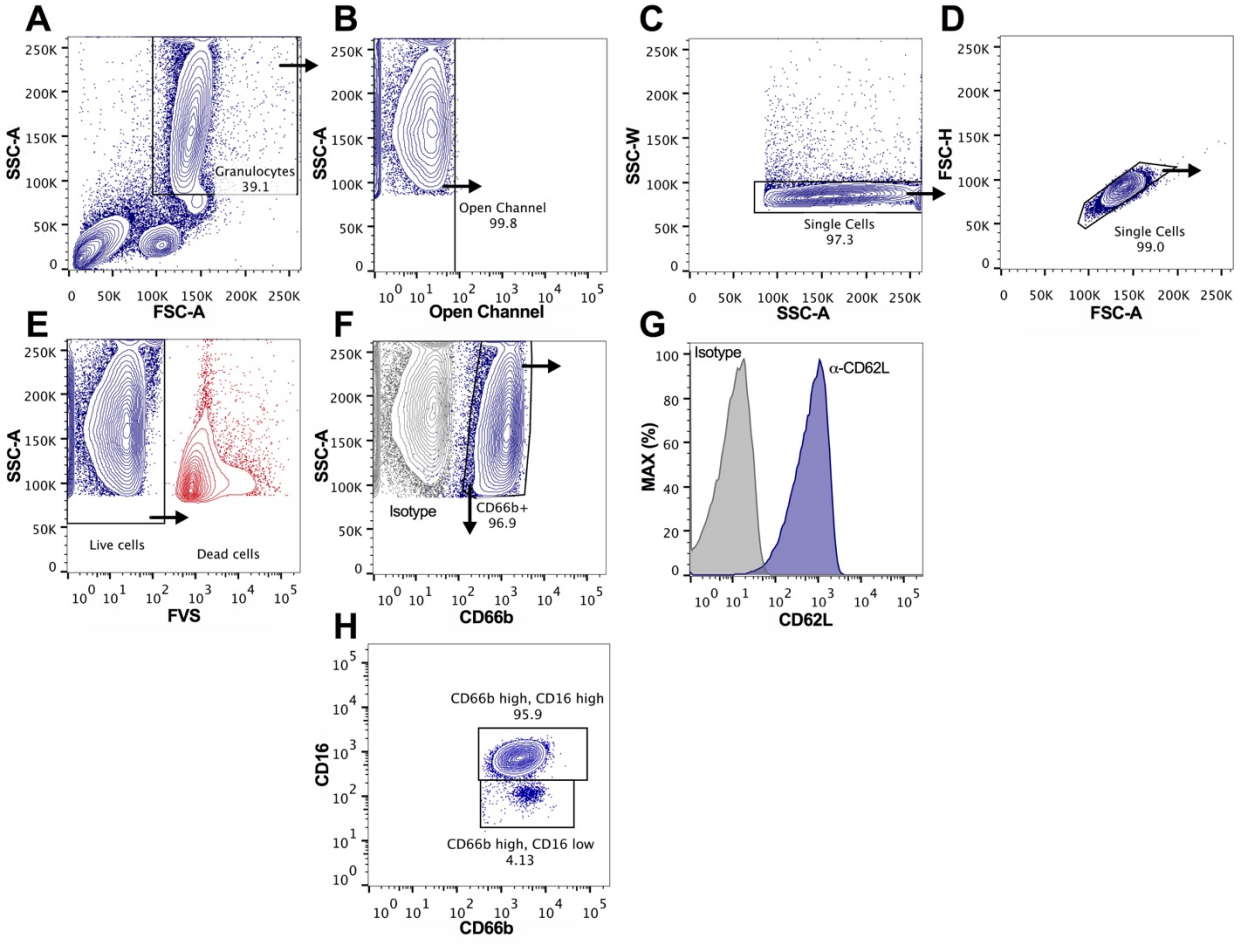

Supplementary Fig. 1. Representative gate strategy used for neutrophils analysis. A classic forward-scatter (FSC) vs side-scatter (SSC) characteristic dot plot was used to select neutrophils population (**A**) from peripheral blood collected from healthy donors and patients. Autofluorescent (**B**) and doublets (**C-D**) were excluded and live cells were selected (**E**). CD66b^{+} positive cells (**F**) were gated and the MFI of surface markers, such as CD62L (**G**) were assessed. Around 96% of CD66b^{+} cells are mature neutrophils (CD66b-high/CD16-high) and 4% of CD66b^{+} cells are CD66b-high/CD16-low, which is suggestive of immature neutrophils or eosinophils (**H**). Approximately 100.000 gated events were collected in each analysis. The analysis was performed in a FACSVerse using FACSuite software (BD Biosciences) and FlowJo software (FlowJo LLC).

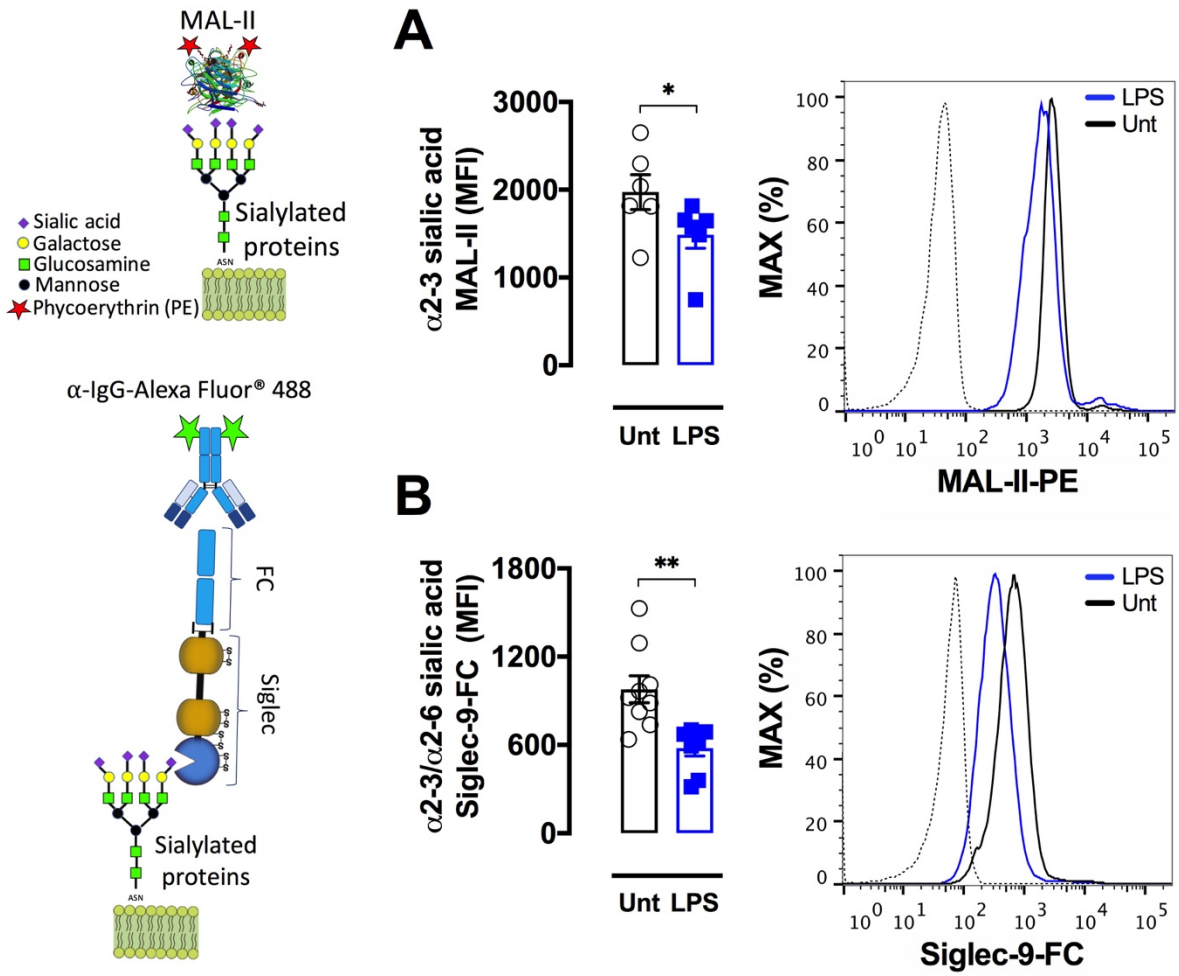

Supplementary Fig. 2. LPS reduces surface α2-3 sialic acids from human neutrophils. Whole blood containing 1 x 10^6 leukocytes from healthy donors were stimulated with 1 µg/mL LPS for 90 min and α2-3 sialic acid contents were assessed by staining cells with biotinylated *Maackia Amurensis* Lectin II (MAL-II) (**A**) followed by streptavidin-phycoerythrin (PE) incubation. Siglec-9 ligands (**B**) were labeled by incubation of chimeric protein containing Siglec-9 sialic acid-Ig binding domain fused to a human IgG-Fc portion (Siglec-9-Fc). Siglec-Fc-9 were incubated with α-IgG1-Alexa Fluor 488 before adding the probe to cells. The MFI was analyzed on $CD66b^+$ cells using the gate strategies shown in Supplementary Fig. 1. *P < 0.05. Symbols represent individual donors and data are shown as mean ± SEM from pooled data of two to three independent experiments (n=6-9). Unt = untreated cells; LPS = lipopolysaccharide; dotted line = unstained cells.

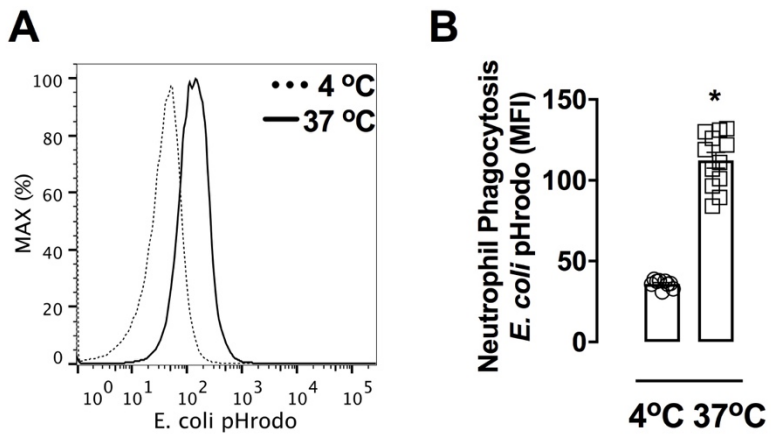

Supplementary Fig. 3. Phagocytosis of *E. coli* pHrodo bioparticles at 4 °C and 37 °C. Total leukocytes (1 x10^6) were incubated with *E. coli* pHrodo bioparticles (100 µg/mL) for 60 min at 4°C or 37 °C and the phagocytosis in viable $CD66b^+$ cells was assessed. Symbols represent individual donors and data are shown as mean ± SEM from pooled data of three to four independent experiments (n = 9-12). **P* < 0.001.

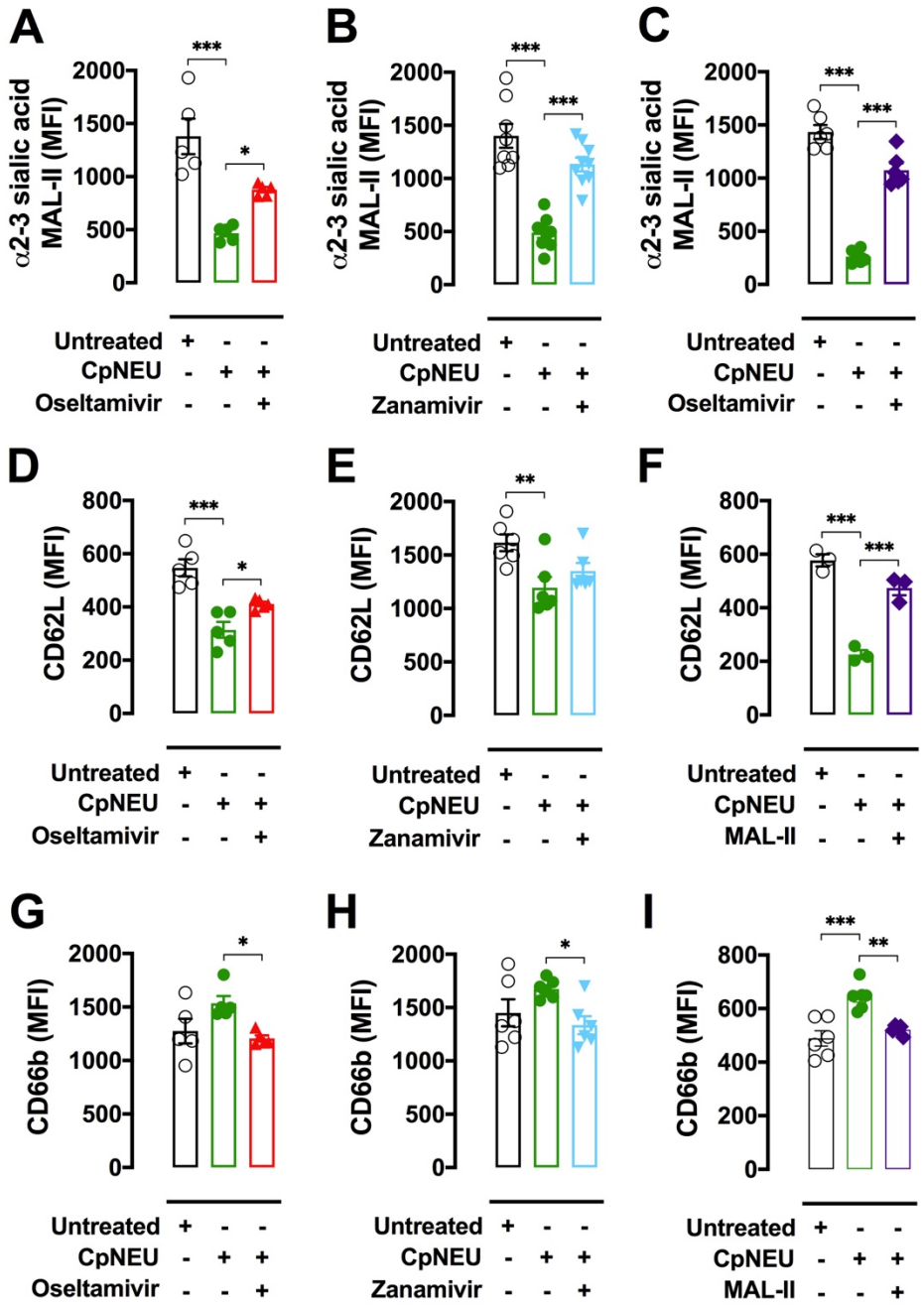

Supplementary Fig. 4. CpNeu-induced human neutrophil activation. Total leukocytes (1 x 10^6) were incubated or not with CpNEU (10 mU, 60 min, 37 °C, 5% CO_2) CpNEU plus Oseltamivir (100 μM), CpNEU plus Zanamivir (30 μM) or CpNEU plus MAL-II (1 μg/mL). Leukocytes were stained with MAL-II to detect α2-3 sialic acids (**A-C**) or with cell activation markers CD62L (**D-F**) and CD66b (**G-I**). The MFI was analyzed on $CD66b^+$ cells. Symbols represent individual donors and data are shown as mean ± SEM

966 from pooled data of two to three independent experiments (n = 5-9) except for F that
967 was made once with n=3. *P < 0.05; **P < 0.01; ***P < 0.001. MAL-II = *Maackia*
968 *amurensis* lectin II; CpNEU = neuraminidase *Clostridium perfringens*.
969

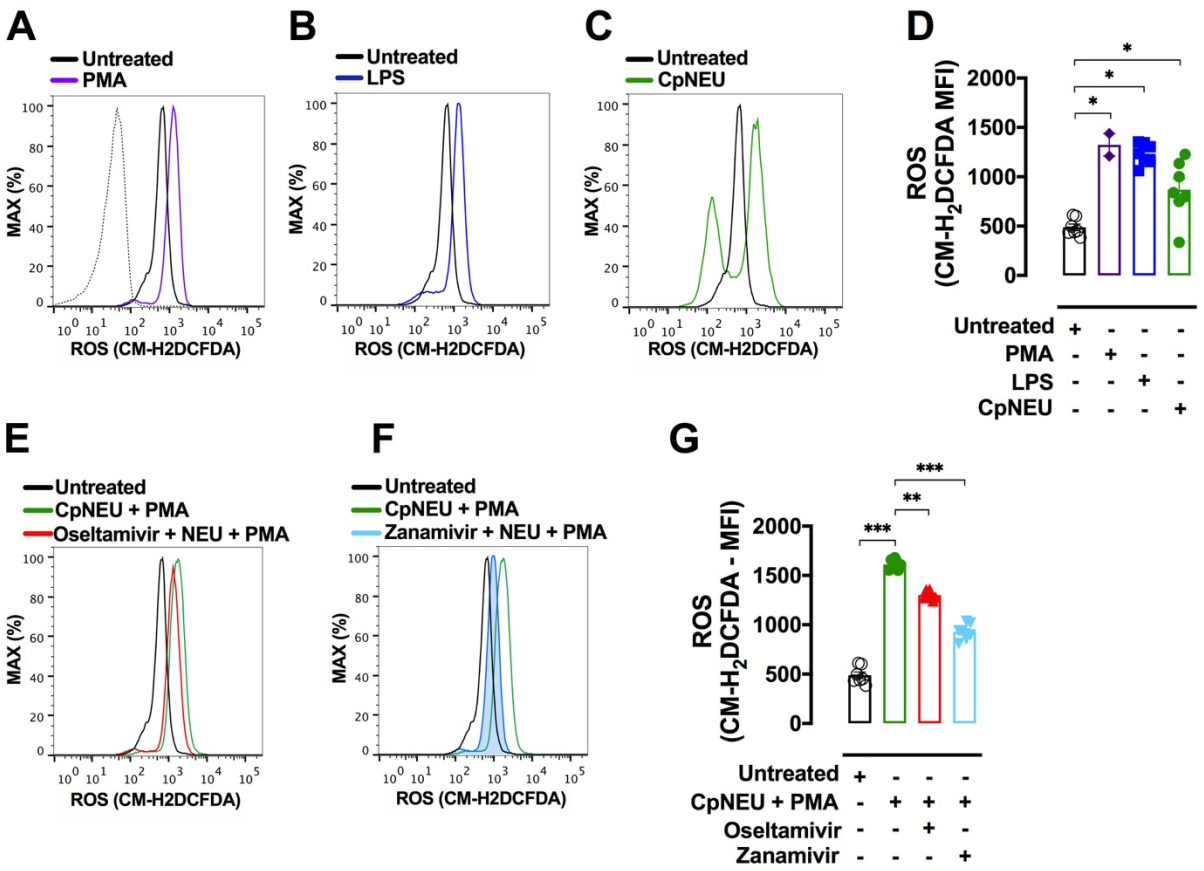

970

971 **Supplementary Fig. 5. ROS production in neutrophils stimulated with LPS,**
972 **CpNEU, or PMA.** Whole blood from healthy donors containing 1 x 10^6 leukocytes were
973 exposed or not to LPS (1 µg/mL, 90 min) (**B and D**). Total leukocytes (1 x 10^6) were
974 incubated or not with CpNEU (10 mU, 60 min) (**C-D**), CpNEU plus Oseltamivir (100 µM)
975 or CpNEU plus Zanamivir (30 µM) (**E-G**). Leukocytes were incubated with 5 µM CM-
976 H2DCFDA fluorescent probe for 15 min and PMA (10 µM) was used to stimulate ROS
977 production for 10 min (**A and E-G**). The MFI was analyzed on $CD66b^+$ cells**.** Symbols
978 represent individual donors and data are shown as mean ± SEM from pooled data of
979 two independent experiments (n = 2-6). **P* < 0.05; ***P* < 0.01; ****P* < 0.001. C = control;
980 CM-H2DCFDA = 5-(and-6)-chloromethyl-2',7'-dichlorodihydrofluorescein diacetate,
981 acetyl ester; LPS = lipopolysaccharide; CpNEU = neuraminidase *Clostridium*
982 *perfringens*; PMA = phorbol 12-myristate 13-acetate.
983

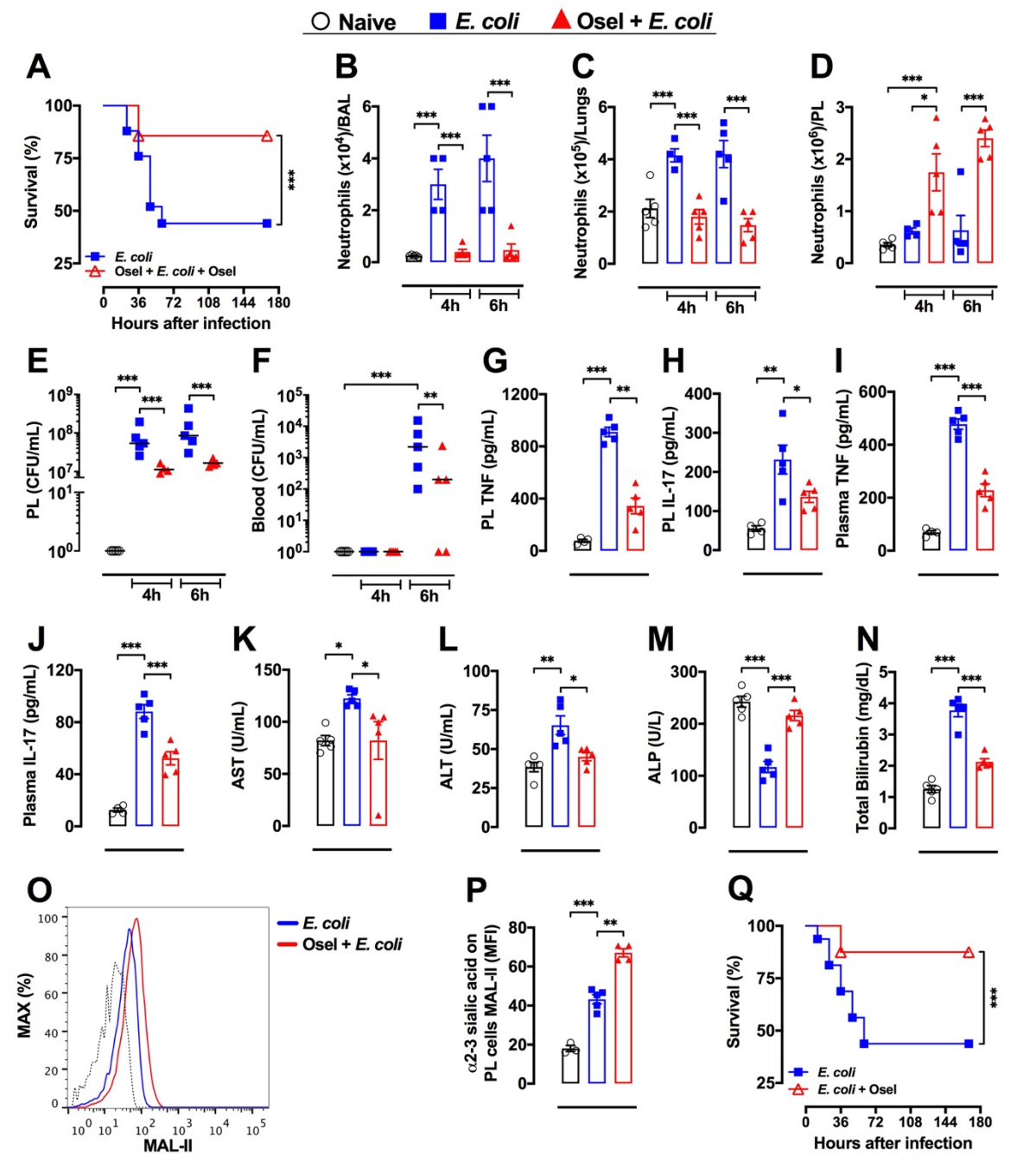

Supplementary Fig. 6. Oseltamivir improved the outcome of *E. coli*-induced sepsis. Sepsis was induced by intraperitoneal (IP) administration of 1 × 10^7 CFU/mice *E. coli* (ATCC 25922). Mice were randomly pretreated *per oral* (PO) via (2 hr before infection) and posttreated (6 hr after infection, 12/12 hr, PO, for 4 days) with Oseltamivir phosphate (Osel, 10 mg/Kg) or saline and their survival rates were monitored over 168 hr (**A,** n=16). In another set of experiments (n=3-5) mice were randomly pretreated (2 hr

before infection) with Oseltamivir phosphate (10 mg/Kg, PO) and the number of neutrophils in bronchoalveolar lavage (BAL, **B**) and in lung tissue (**C**) was counted. In peritoneal lavage (PL) infiltrating neutrophils counts (**D**), TNF (**G**), IL-17 (**H**) and the number of colony-forming units (CFU) in PL (**E**) or blood (**F**) were determined 4 or 6 hr after infection. Plasma levels of TNF (**I**), IL-17 (**J**), AST (**K**), ALT (**L**), ALP (**M**) and total bilirubin (**N**) were evaluated. The amount of surface α2-3 sialic acids were also assessed in PL SSC^{high}/$Gr\text{-}1^{high}$ cells as shown by the representative histograms (**O**) or MFI (**P**); dotted line = unstained cells. Mice were also randomly posttreated (starting 6 hr after infection, 12/12 hr, PO, for 4 days) with saline or Oseltamivir phosphate (10 mg/Kg) and their survival rates were monitored over 168 hr (**Q**). The results are expressed as percent of survival (n=16), mean or median (only for FACS data) ± SEM. **P* < 0.05; ***P* < 0.01; ****P* < 0.001. These experiments were repeated 3 times for survival analysis and twice for other parameters. Osel = Oseltamivir; AST = alanine aminotransferase; ALT = aspartate aminotransferase; ALP = alkaline phosphatase; MAL-II = *Maackia amurensis* lectin II.

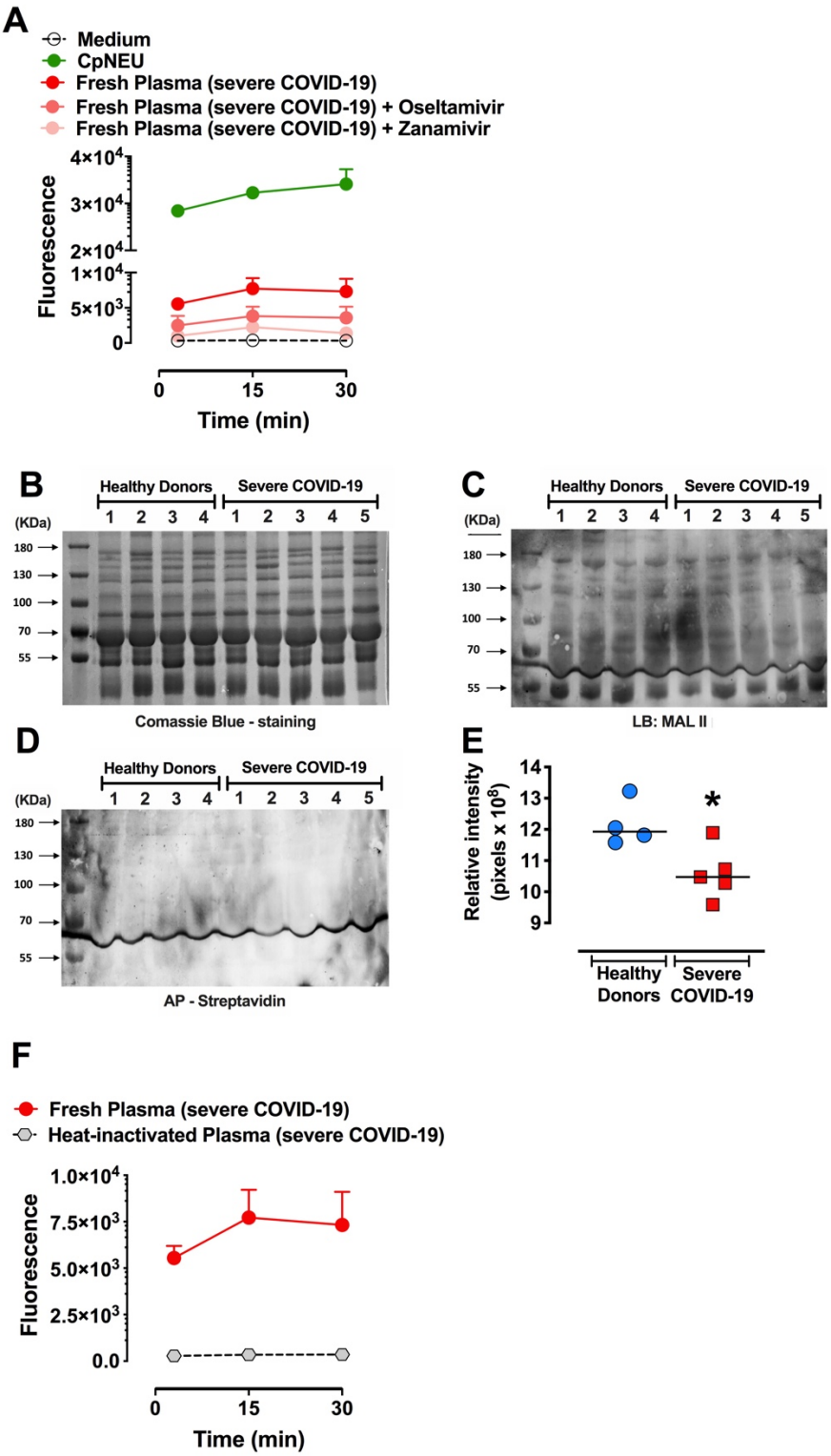

Supplementary Fig. 7. NEU activity is increased in plasma from severe COVID-19 patients. NEU activity was evaluated in fresh plasma from severe COVID-19 patients in the presence or absence of Oseltamivir (100 µM) or Zanamivir (30 µM) (**A**) and in heat-

inactivated plasma from COVID-19 patients (**F**). Neuraminidase isolated from *Clostridium perfringens* (CpNEU) was used to validate the NEU activity assay. Twelve µg of total serum proteins from healthy donors (n=4) or severe COVID-19 patients (n=5) were separated by SDS-PAGE 10% and stained with coomassie blue (**B**). Lectin blotting (LB) were performed with biotin-conjugated MAL-II for staining α2-3 sialic acid-containing proteins **(C)** or membrane were incubated with AP-Streptavidin without MAL-II (as a control) **(D).** The intensity of lectin staining of each lane was evaluated and normalized to the total proteins on corresponding gel lanes **(E)**; *p=0.02 Unpaired t test - Welch's correction**.** MAL-II = *Maackia amurensis* lectin II; CpNEU = neuraminidase *Clostridium perfringens*.

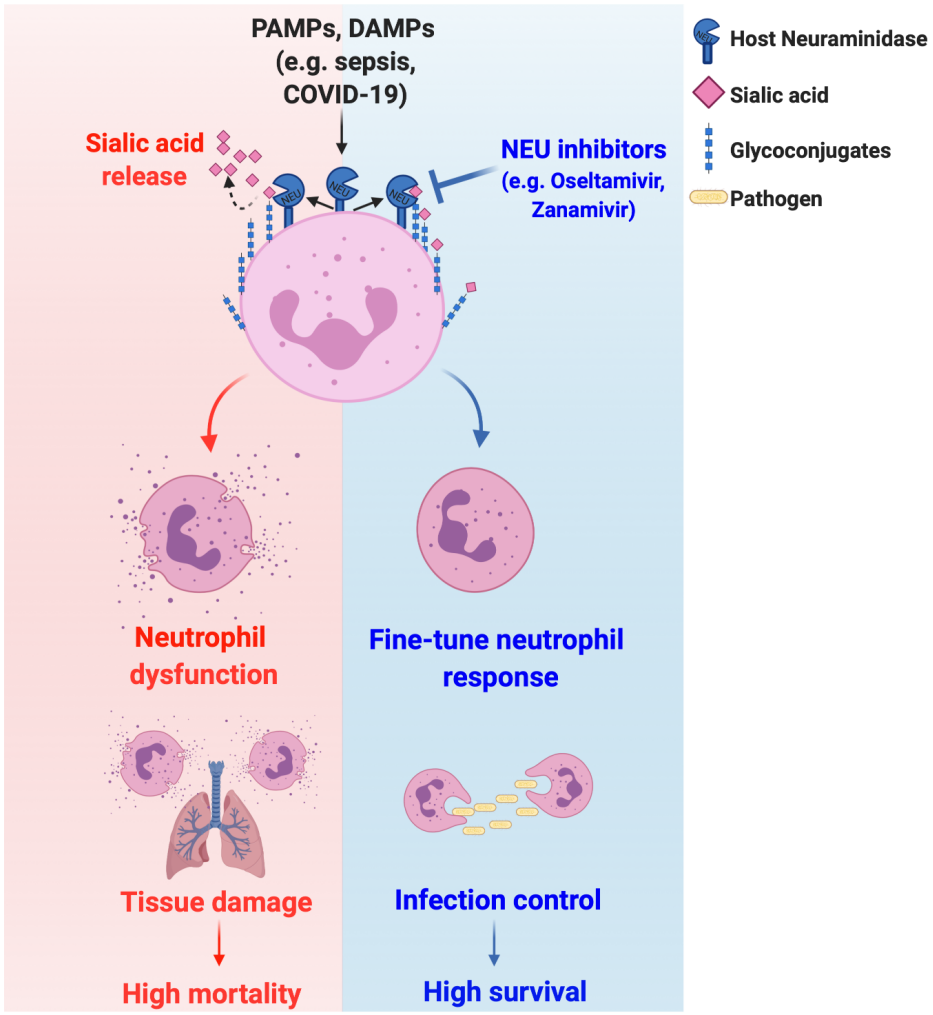

Supplementary Fig. 8. Working model. PAMPs and DAMPs in severe diseases such as sepsis and COVID-19 lead to neuraminidase activation with shedding of surface sialic acid and neutrophil overactivation, resulting in tissue damage and high mortality rates. On the other hand, neuraminidase inhibitors (e.g., Oseltamivir, Zanamivir) prevent the sialic acid release to regulates neutrophil response, resulting in infection control and high survival rates.

1032 **Supplementary Table 1.**

1033

1034 **Supplementary Table 1. Clinical information of samples from UFSC University**
1035 **Hospital, SC, Brazil**

1036

	Severe COVID-19	***Convalescent COVID-19***
Characteristic		
Gender (Male/Female)	3/2	7/5
Age (years)	44.4 (25;65)	53.2 (36;80)
Weight (kilos)	90.0 (62.2;127)	85.1 (51.8;150)
Height (m)	1.72 (1.65;1.8)	1.7 (1.55;1.83)
Cough	4 (80%)	8 (66.7%)
Dyspnea	4 (80%)	5 (41.7%)
Chest Pain / Oppression	1 (20%)	4 (33.3%)
Asthenia	2 (40%)	3 (16.7%)
Myalgia	3 (60%)	3 (16.7%)
Anosmia	1 (20%)	5 (41.7%)
Ageusia / Dysgeusia	1 (20%)	4 (33.3%)
Fever	3 (60%)	3 (16.7%)

Paresthesia	0 (0%)	0 (0%)
Headache	0 (0%)	2 (16.7%)
Diarrhea	0 (0%)	1 (8.3%)
Diabetes mellitus	3 (60%)	4 (33.3%)
Systolic BP (mmHg)	132.2 (100;150)	126.4 (100;177)
Diastolic BP (mmHg)	84.2 (80;90	78.55 (60;102)
Heart rate (bpm)	96.4 (80;115)	86.4 (72;115)
Respiratory frequency (bpm)	20.8 (18;25)	20.8 (11;29)
Length of hospitalization (days)	6.6 (4;10)	8.3 (3;16)
Mechanical ventilation	0 (0%)	3 (16.7%)
Mechanical ventilation time (days)	0 (0%)	7.3 (5;9)
Saturation (O2%)	90.4 (85;97)	93.3 (86;99)
SOFA Score	0.17 (0;1)	0.6 (0;2)

Laboratory data		
Hemoglobin (g/dL)	13.5 (11;15)	13.65 (11.3;15.7)
Hematocrit (%)	40 (33.4;47.1)	40.2 (34.8;45.5)

Leukocytes (/μL)	7988 (4070;12930)	8098 (5330;10660)
Neutrophils (/μL)	5731 (3355;10098)	6448.5 (3923;9135)
Lymphocytes (/μL)	1526 (451;3728)	955.8 (208;1687)
Monocytes (/μL)	369 (253;483)	473.2 (168;961)
Platelets (x10^3/μL)	235 (115:314)	238 (117;436)
PCR (mg / dL)	52.5 (22;78.7)	90.7 (15;214)

Supplementary Table 2. Clinical information of samples from Hospital Naval Marcílio Dias, RJ, Brazil

	Severe COVID-19
Characteristic	
Gender (Male/Female)	2/3
Age (years)	66 (55-73)
Cough	4 (80%)
Dyspnea	4 (80%)
Chest Pain / Oppression	0 (0%)
Asthenia	1 (20%)
Myalgia	2 (40%)
Anosmia	2 (40%)
Ageusia / Dysgeusia	0 (0%)
Fever	4 (80%)
Paresthesia	0 (0%)
Headache	0 (0%)
Diarrhea	3 (60%)

Diabetes mellitus	3 (60%)
Systolic BP (mmHg)	141.4 (108;166)
Diastolic BP (mmHg)	74.8 (51;100)
Heart rate (bpm)	83.8 (57;102)
Respiratory frequency (bpm)	24 (14-40)
Length of hospitalization (days)	32.8 (10;90)
Mechanical ventilation	5 (100%)
Saturation (O2%)	87.3 (83;91)

Laboratory data	
Hemoglobin (g/dL)	11.92 (7.9;13.3)
Hematocrit (%)	35.72 (23;41.6)
Leukocytes (/µL)	7900 (5400;12100)
Neutrophils (/µL)	5724.8 (4266;7502)

Lymphocytes (/μL)	983.8 (430;1694)
Monocytes (/μL)	575.8 (216;1452)
Platelets (x10^3/μL)	172.8 (109;219)
PCR (mg / dL)	15.8 (5.16;26.8)

1043
1044